Distribution of seasoning agents with different characteristics onto food gel

Yuki Sha

2017

Contents

General introduction

Many food contain polymers, often forming a gel-like matrix. Some foods are even regarded as gels themselves. For example, rice cakes, boiled eggs, sausages, and konjac jelly, are gels consisted with starch, heat-induced egg protein (Hatta *et al.*, 1986; Doi, 1993; Handa *et al.*, 1998), meat proteins cross-linked by transglutaminase (Motoki and Seguro, 1998; Kuraishi *et al.*, 2001; Gerrard, 2002; Ahhmed, 2007; 2009), and polysaccharides (Kato and Matsuda, 1969; Maekaji, 1974; Zhang *et al.*, 2001), respectively.

Different polymers express different chemical and electrical properties. For example, starch is an electrically neutral polymer composed of a single kind of monomer, glucose, while proteins can be regarded as amphoteric polymers constructed using 20 different amino acids. Some polysaccharides, such as alginic acid, carrageenan, or agarose, express a negative charge because of carboxylic (Gacesa, 1988), sulfonic (De Ruiter and Rudolph, 1997; Campo *et al.*, 2009), or pyruvic (Fatin-Rouge *et al.*, 2003) substitutes on their major chains. Thus, starch, protein, and alginate gels are regarded as size exclusion polymer, amphoteric-ion exchanger and cation exchanger, respectively.

Generally, low-molecular-mass compounds are used in the seasoning of food. However, their chemical or electrical properties are different each other. For example, sucrose, used in enhancing the sweetness of food, is a non-electrolyte, sodium chloride, which is used to enhance saltiness is a strong electrolyte, while acetic acid (sour taste) is a weak electrolyte. Besides, most of bitter compounds exhibit high hydrophobicity (Fox, 1932; Belitz and Wieser, 1985; Ishibashi *et al.*, 1988). Therefore, many interactions, such as size exclusion, ion exchange and hydrophobic interaction, occur during the seasoning of food. The seasoning process is characterized by two factors: the distribution of a seasoning compound onto the food gel and the diffusion of the compound in the gel. The distribution determines the final concentration of the compound in the gel, while the diffusion regulates the time required by the gel to reach an equilibrium state.

Some studies reported diffusion of solutes in food polymer gel, such as effective diffusion coefficient of glucose in κ-carrageenan gel (Nguyen and Luong, 1986), glucose and amino acid in alginate gel (Tanaka *et al.*, 1984) and sodium chloride in agar gel (Odake *et al.*, 1990). From the point of practical food processing, diffusion of glucose and salts in beef and pork (Djelveh and Gros, 1988), and of salt in white cheese (Turhan and Kaletunç, 1992) were evaluated.

Distribution of a solute onto food matrix plays an important role in seasoning process as well as diffusion. As above-mentioned, food gel matrixes and seasoning compounds are inherently different in their electrical properties. There are many combinations between food matrixes and seasoning compounds. However, systematical study would scarcely have been conducted on distribution of seasoning compounds to food matrixes.

In order to propose a reasonable food seasoning process, it is indispensable to predict the amounts of seasoning compounds finally absorbed on food and time required for seasoning. However, above-mentioned diversity of chemical and electrical nature in food polymer and seasoning agents makes the prediction complicate.

Our laboratory has reported that swelling pressure of ion-exchange resin plays an important role on distribution equilibrium of saccharides onto the resin (Adachi *et al.*, 1989; Adachi and Matsuno, 1997). We apply swelling pressure to food polymer gel in order to predict distribution equilibrium of seasoning agents onto them.

Insights obtained from this study would make a great progress in food seasoning process, in other words, determining the concentration of seasoning liquid and time required for immersing food materials into seasoning liquid.

In Chapter 1, starch gel was used as a typical food model gel, since starch is electrically neutral polymer consisted only with glucose residue. At first, the distribution coefficients of non-electrolytes onto starch gel were measured. Subsequently, relationship between the distribution coefficients and molar volume of each non-electrolytes was discussed. In this chapter, swelling pressure was introduced. Diffusion coefficients of seasoning agents with

various chemical nature were also measured, and the tortuosity factor of starch gel was discussed.

In Chapter 2, insights obtained in Chapter 1 was applied to distribution of saccharides onto rice, which is mainly composed with starch. Four cultivars of rice, which is different from each other in amylose content, were used. Effect of temperature on distribution coefficient of fructose onto rice was also assessed.

In Chapter 3, we focused on the role of hydrophobic interaction on distribution of seasoning agents onto food gel. In order to investigate in a model system, measurements of adsorption isotherms of five kinds of hydrophobic substances onto chromatographic organic monolith were conducted.

In Chapter 4, effects of eluent and counter-ion form of polymer gel on distribution coefficients of saccharides were focused on. In this research, we used a cation-exchange resin for a model of food polymer gel. Aqueous ethanol was used as eluent, and effects of ethanol concentration on distribution coefficients of saccharides onto a cation-exchange resin were evaluated.

Chapter 1

Swelling pressure of tapioca starch gel estimated from distribution coefficients of non-electrolytes

1.1. Introduction

In this chapter, a starch gel, an elementary food gel-model, was used for analysis. Starch is a homopolymer, comprising of glucose residues linked by α-1,4-glycosidic bonds (Pigman, 1970), and is therefore regarded as an electrically neutral polymer. At first, the effects of temperature on the apparent density and porosity of starch gel were evaluated. Subsequently, the distribution coefficients of non-electrolytes on the starch gel were measured at a temperature range of 25°C to 60°C, in order to estimate the swelling pressure of the gel at each temperature. The distribution coefficients of electrolytes were also measured. Finally, the distribution and diffusion coefficients of typical seasoning compounds, exhibiting different chemical properties on or within the gel, were measured.

1.2. Materials and methods

1.2.1. Materials

Dried spherical tapioca beads (Youki Food, Tokyo, Japan) were purchased from a supermarket in Kobe, Japan. Ethylene glycol, glycerol, glucose, fructose, sucrose, and raffinose pentahydrate were purchased from Wako (Wako Pure Chemical Industries, Osaka, Japan). Sodium hydrogen L(+)-glutamate monohydrate, vanillin, glucose CII-test kit, and invertase (obtained from yeast) were also purchased from Wako. Other chemicals were purchased from Wako or Nacalai Tesque Inc. (Kyoto, Japan).

1.2.2. Preparation of starch gel

Five grams of dried tapioca beads were rehydrated for 20 min in 500 mL of boiling water

in an Erlenmeyer flask, with gentle stirring using a magnetic stirrer to prevent sedimentation of the beads. The beads were then quickly removed from the boiling water and washed with 1 L of pre-cooled water. The beads were soaked in a large quantity of water for at least 3 h to attain equilibrium at 25°C. The radii of the tapioca beads before and after rehydration were *ca*. 1.4 and 3.0 mm, respectively. The beads are hereafter denoted as starch gel, or merely "the gel."

1.2.3. Apparent density and porosity of starch gel

The gel was equilibrated in distilled water at varying temperatures (25, 40, 50, 60, or 80°C), using a temperature-controlled water bath (SDminiN or SD, Taitec, Saitama, Japan) and a cooler (Cool Way 100, Gex Corporation, Osaka, Japan) for at least 2 h. Apparent density of the starch gel was pycnometrically determined. The gel was dried at 105°C for 5 days using a constant temperature oven (DN-400, Yamato Scientific, Tokyo, Japan). The difference between dry and wet weights of the gel was divided by density of water to estimate the pore volume of the gel. Porosity, which was defined as a ratio of water volume in the gel to the whole gel volume, was calculated by dividing the pore volume with the whole gel volume.

1.2.4. Distribution coefficient on the starch gel

Distribution coefficient of a solute on the gel was measured by using an adsorption-desorption process. Briefly, 1 g of the gel was precisely weighed and soaked in 15 mL of a solution (containing a specific solute; concentration ranging from 0.1% (w/v) to 15% (w/v)). The gel was incubated until a distribution equilibrium was achieved (6 h or longer), and subsequently removed from the solution. The excess solution on the gel surface was blotted using a Kimtowel (Nippon Paper Crecia, Tokyo, Japan). The gel was then soaked in 2 mL of distilled water in order to desorb the solute, for 6 h or longer. The concentrations of non-electrolytes and electrolytes were determined using a pocket refractometer (PAL-1, Atago, Tokyo, Japan) and pocket salinometer (PAL-ES1, Atago), respectively. The concentrations of

acetic acid and monosodium glutamate were also analyzed using the refractometer and salinometer, respectively. The vanillin concentration was determined by measuring the absorbance at 280 nm, using a UV-1200 spectrophotometer (Shimadzu, Kyoto, Japan).

Mass balance for a solute before and after desorption was expressed using Eq. (1.1).

$$(W_g / \rho_{app})\, C_0\, K_{app} = (W_g / \rho_{app})\, C_f\, K_{app} + V_L\, C_f \qquad (1.1)$$

where, C_0 [mol/m^3] is the solute concentration of the outer solution for adsorption, C_f [mol/m^3] is the solute concentration of the outer solution after desorption, V_L [m^3] is the volume of distilled water used for desorption, and W_g [kg] is the weight of starch gel. Equation (1.1) can be re-written as follows:

$$C_f = K_{app}\, [((W_g / \rho_{app}) / V_L] \cdot (C_0 - C_f) \qquad (1.2)$$

When the distribution coefficient, K_{app} [-], is independent of the solute concentration, the plot of C_f against $[(W_g/\rho_{app})/V_L] \cdot (C_0 - C_f)$ produce a straight line passing through the origin, and the K_{app} value is obtained from the slope of this line.

1.2.5. Diffusion coefficient in starch gel

The gel was immersed in an excess volume of 30 mmol/L glucose, 30 mmol/L sucrose, 500 mmol/L NaCl, 500 mmol/L monosodium glutamate, 800 mmolL acetic acid, or 10 mmol/L vanillin, in order to attain a distribution equilibrium. The diffusion coefficient was then measured using a desorption method described in previous studies (Horowitz and Fenichel, 1964; Nakanishi *et al.*, 1977; Westrin *et al.*, 1994).

The concentrations of NaCl, monosodium glutamate, and acetic acid were determined using an electrical conductivity meter (CD-35MII, M & S Instruments, Osaka, Japan). The concentration of vanillin was determined as mentioned in the previous section. The concentration of glucose was measured with the glucose CII-test kit. Sucrose was hydrolyzed by invertase; the invertase solution was diluted in 50 mmol/L acetate buffer (pH 5.0) to a concentration of 0.016 U/L and 1 mL of the sucrose solution was mixed with 20 μL of this

diluted invertase solution. Following the complete hydrolysis of sucrose, the glucose produced was analyzed with the glucose CII-test kit.

1.2.6. Differential scanning calorimetry (DSC) measurement

Distilled water (6 times the weight of tapioca beads) was added to the beads. The beads were ground into a paste with a mortar and pestle. The sample (10 mg) was precisely weighed using a thermogravimeter (TGA-50, Shimadzu) and sealed in a disposable cell constructed of aluminum. The sample-containing cell was heated to 95°C from the ambient temperature at a rate of 5 °C/min, using a differential scanning calorimeter (DSC-50, Shimadzu). The same quantity of distilled water was used as a reference.

1.2.7. Ash analysis

Dry tapioca beads were incinerated in a crucible (treated at 550°C for 2 h) using an electrical furnace (SH-OMT-II, Nitto Kagaku, Nagoya, Japan), maintained at 600°C for 2 h, in order to determine the ash content.

A qualitative analysis of the ash was also performed. The ash (0.031 g) was dissolved in a 1.0 mL HCl and 0.5 mL nitric acid mixture, and diluted up to 25 mL using distilled water. The elements present in the ash were analyzed using an ICP emission spectrometer (ICP-8100, Shimadzu), at volumetric flow rates of coolant, plasma, and carrier gases of 14 L/min, 1.2 L/min, and 0.70 L/min, respectively.

1.3. Results and discussion

1.3.1. Temperature dependence of apparent density and porosity of starch gel

Figure 1.1 displays the apparent density ρ_{app} and porosity ε_p of starch gel at various temperatures. The ρ_{app} was lower and the ε_p was greater at a high temperature. These results suggested that the starch gel swells more at higher temperatures. Water regains of the starch gel

were 1159 ± 3, 1125 ± 10, 1575 ± 38, 1382 ± 17 and 1986 ± 23 g-water/g-dry gel at 25, 40, 50, 60 and 80°C, respectively, also indicating swelling more at higher temperature. However, the ε_p value at 60°C was slightly lower than that at 50°C.

1.3.2. Estimation of swelling pressure of starch gel

Figure 1.2 shows the C_f vs. $[(W_g/\rho_{app})/V_L]\cdot(C_0 - C_f)$ plots for ethylene glycol, glucose, and raffinose at 25°C and 50°C. The plots for each solute at a specific temperature produced a straight line passing through the origin, and the K_{app} value was calculated from the slope of the line. Other non-electrolytes also produced straight lines passing through the origin. Lower K_{app} values were observed for non-electrolytes with a larger molecular mass. The K_{app} values, which were lower than the ε_p values of the gel, indicated the effect of a factor other than the steric effect of the gel matrix on the distribution of non-electrolytes on the gel.

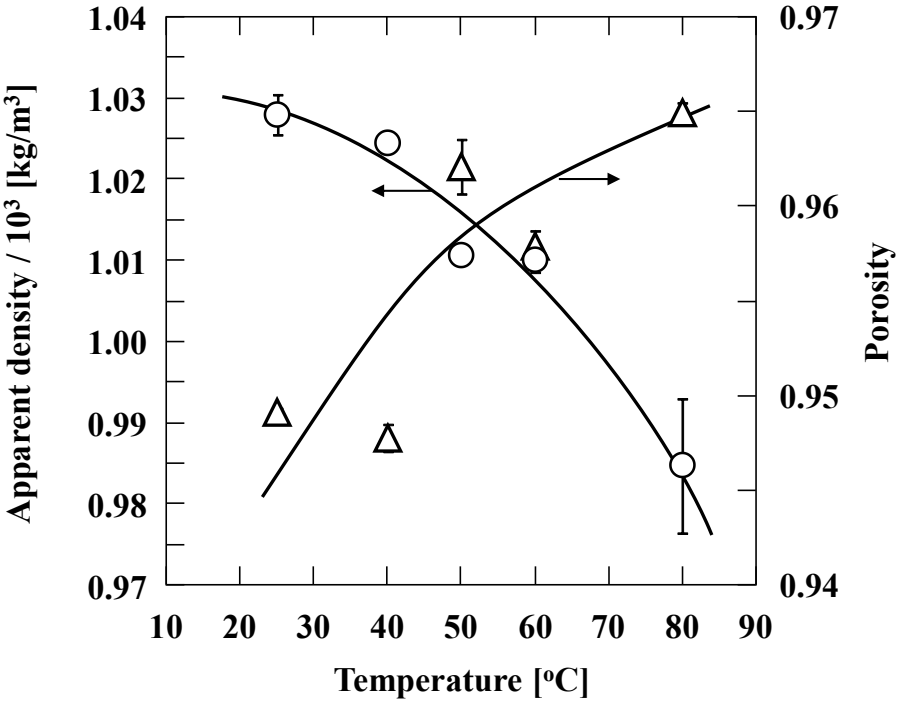

Fig. 1.1. Apparent density (○) and porosity (△) of the starch gel at various temperatures. The values are shown as mean ± standard deviation (SD) (n = 3).

We have previously reported that the K_{app} of a non-electrolyte on a cation-exchange resin can be expressed by Eq. (1.3), by taking into consideration the swelling pressure of the resin, Π [Pa] (Adachi *et al*., 1989).

$$K_{app} = \gamma_0 \exp[-\Pi v_S / (RT)] \quad (1.3)$$

where R [J/(mol·K)] is the gas constant, T [K] is the absolute temperature, v_S [m^3/mol] denotes the partial molar volume of a solute. γ_0 [-] represents a parameter including the ratio of the activity coefficient of a solute in the outer solution phase to that in the resin phase, and the steric effect on the distribution of a solute on the resin.

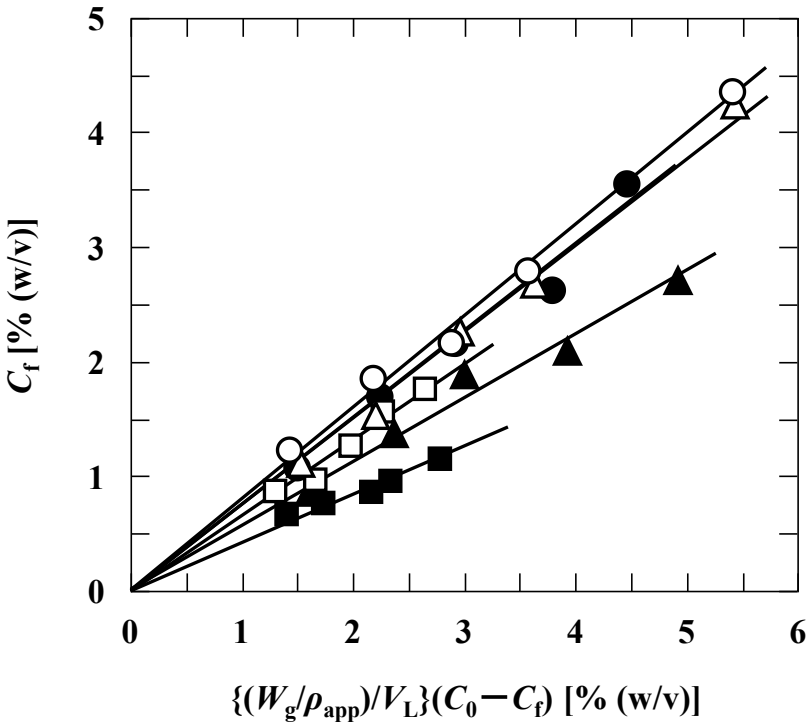

Fig. 1.2. Relationship between C_f and $[(W_g/\rho_{app})/V_L]\cdot(C_0\text{-}C_f)$ for ethylene glycol (○, ●), glucose (△, ▲), and raffinose (□, ■) at 25°C (open symbols) and 50°C (closed symbols).

Equation (1.3) was applied to estimate the swelling pressure of the starch gel. For this, we used the molar volume of each solute instead of the partial molar volume. Briefly, a radius of a hydrated solute, r_S [m], was estimated from the diffusion coefficient at 25°C (Hayduk and Laudie, 1974; Ribeiro *et al.*, 2006) using the Stokes-Einstein equation (Eq. (1.4)). The molar volume of the solute was assuming that the solute is spherical.

$$D_0 = k_B T / (6\pi \mu r_S) \quad (1.4)$$

where D_0 [m^2/s]is the diffusion coefficient in dilute solution, k_B [J/K] is the Boltzmann constant, and μ [Pa·s] is the viscosity of water.

The molar volumes of ethylene glycol, glycerol, fructose, glucose, sucrose, and raffinose were 0.024, 0.046, 0.114, 0.121, 0.259, and 0.456 L/mol, respectively. The molar volumes were assumed to be constant in the tested temperature range.

The K_{app} values of the non-electrolytes at various temperatures were plotted on a semi-logarithmic scale against their molar volumes (Fig. 1.3). The plots (at all temperatures) produced a straight line, and the swelling pressure of the starch gel at each temperature was estimated from the slope of the line. The Π values of the gel at 25, 40, 50, and 60°C were evaluated to be 1.1, 1.6, 2.9, and 1.7 MPa, respectively. As shown in Fig. 1.4, theΠ value increased with the increase in temperature from 25 to 50°C, but decreased at 60°C. The enthalpy change, ΔH [J/mol], for the swelling was estimated from the swelling pressures at a temperature range of 25°C to 50°C using the van't Hoff equation (Eq. (1.5)), to be 29.9 kJ/mol, indicating the swelling of the gel to be endothermic.

$$\mathrm{d}\ln\Pi / \mathrm{d}(1/T) = -\Delta H / R \quad (1.5)$$

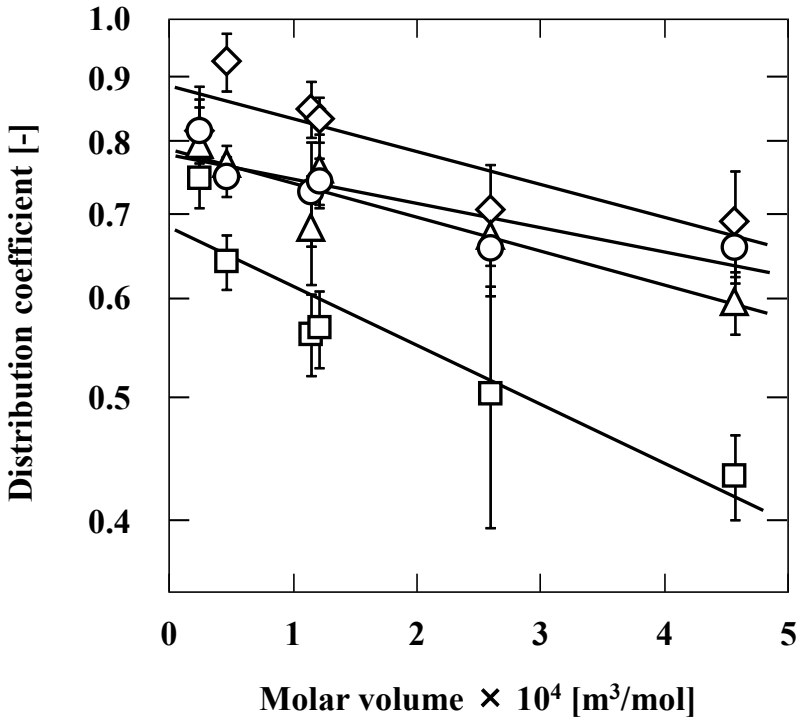

Fig. 1.3. Estimation of swelling pressure of the starch gel at 25°C (○), 40°C (△), 50°C (□), and 60°C (◇) using Eq. (1.3). The solutes used were ethylene glycol, glycerol, fructose, glucose, sucrose, and raffinose.

1.3.3. DSC measurement

Figure 1.5 displays the DSC curve of the tapioca gel. The DSC curve shows two endothermic peaks. The former peak would be ascribed to the gelatinization of starch and the latter one might be caused by the transition of complex between amylose and lipid (Eliasson, 1994). The onset, peak, and conclusion temperatures of the gelatinization process were 63°C, 73°C, and 78°C, respectively. The enthalpy of the gelatinization reaction was calculated to be -3.13 J/g. The onset of gelatinization was at a temperature range of 60°C, at which a decrease in the swelling pressure was observed in previous experiments. Therefore, the lower swelling pressure at 60°C was ascribed to the gelatinization of the tapioca starch. It was suggested that gelatinization of starch gel played an important role in distribution of seasoning compounds to the gel.

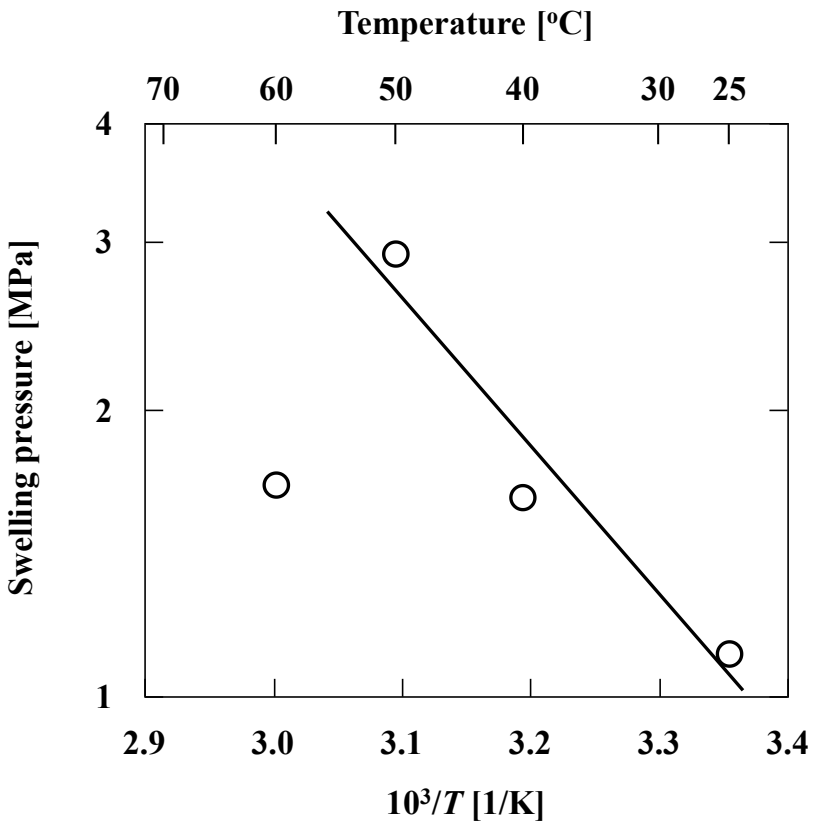

Fig. 1.4. Temperature dependence of the swelling pressure of starch gel.

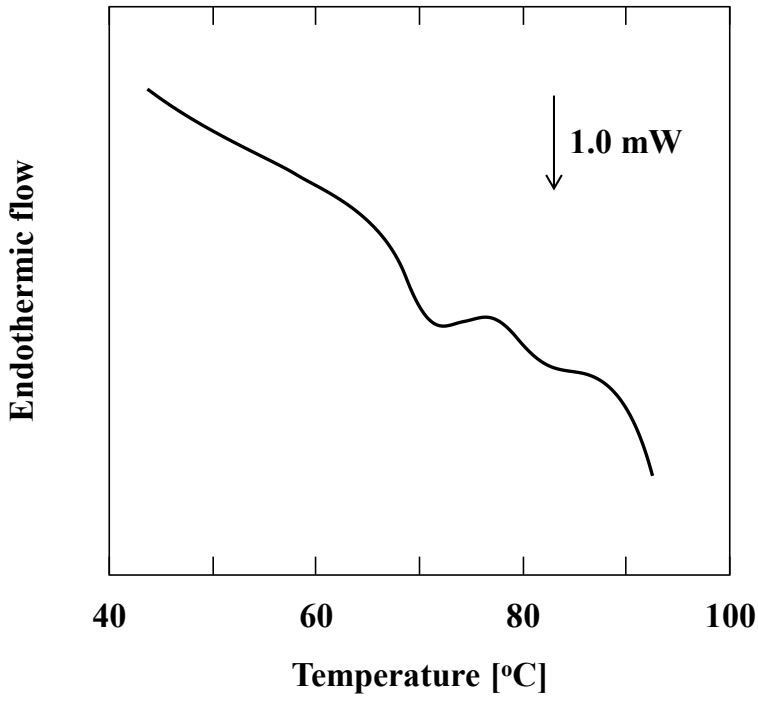

Fig. 1.5. Differential scanning calorimetry curve for tapioca starch.

Starch gel incubated at 25°C for several hours was also analyzed by DSC under the same condition. The DSC curve showed no peak (data not shown), suggesting that the retrogradation of the gel did not occur when soaking in distilled water at 25°C.

1.3.4. Distribution coefficient of electrolyte on starch gel

The K_{app} values of seven electrolytes were measured at 25°C, and were plotted against the molar volumes of the electrolytes in Fig. 1.6. The molar volume of each electrolyte was estimated under the following assumptions: the larger cation and anion in the electrolyte governs the distribution of the electrolyte on the gel due to the electro-neutrality in the gel phase. The molar volumes of hydrated lithium, sodium, potassium, cesium, fluoride, chloride, bromide, and iodide ions were estimated from their diffusion coefficients in dilute aqueous solution (Li and Gregory, 1974) to be 0.034, 0.016, 0.0049, 0.0042, 0.012, 0.0044, 0.0046, and 0.0047 L/mol. For example, the molar volume of NaCl was assumed to be 0.016 L/mol because the molar volume of sodium ion (0.016 L/mol) is larger than that of chloride ion (0.0044 L/mol).

When there is no interaction between a solute and the starch gel, the distribution of the solute on the gel at a specific temperature should be determined using the swelling pressure of the gel and the molar volume of the solute. The solid line in Fig. 1.6 represents the molar volume dependence calculated from Eq. (1.3), using the swelling pressure of the gel at 25°C (1.1 MPa). All the plots were observed to lie under the curve, indicating that any factor could participate in the distribution of electrolyte on the gel.

The ash content of the starch gel was 73 ± 23 mg/100 g-wet sample. The analysis using the ICPS-8100 led to the detection of 19 elements, and the major elements were listed in Table 1.1. The presence of alkali and alkaline earth metals in the starch gel suggested the effect of a weak electrostatic interaction on the distribution of electrolytes on the gel.

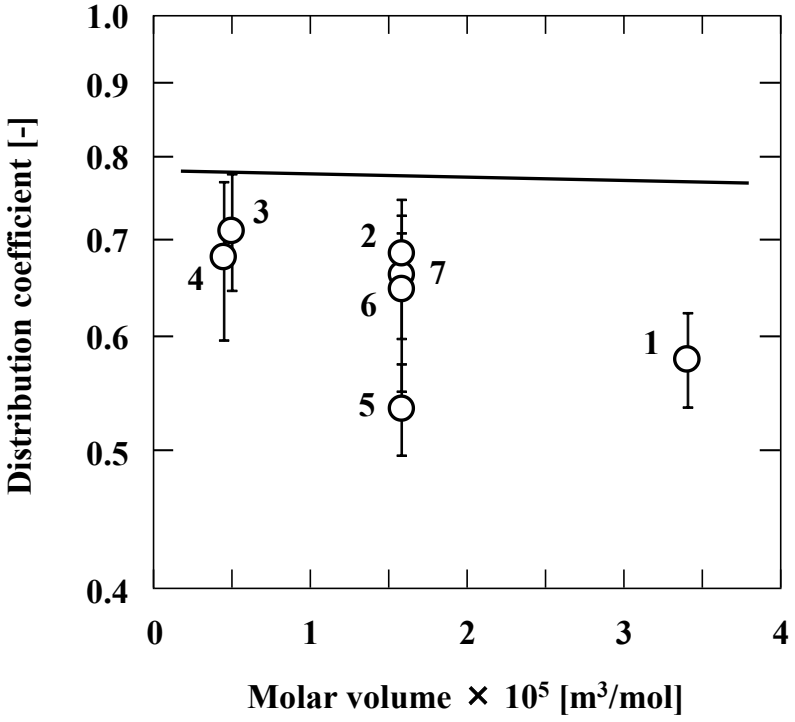

Fig. 1.6. Distribution coefficients of electrolytes at 25°C. Numbers represent the electrolytes used: 1: LiCl, 2: NaCl, 3: KCl, 4: CsCl, 5: NaF, 6: NaBr, and 7: NaI. The values are represented as mean ± SD.

Table 1.1. Ash content of tapioca starch.

	Content [% (w/w)]
Sodium, Na	9.22
Magnesium, Mg	3.45
Calcium, Ca	21.8
Phosphorous, P	8.76
Sulphur, S	2.69
Potassium, K	7.34

It is known that Sephadex, dextran gel cross-linked with epichlorohydrin, contains a few carboxylic groups originated from terminal aldehyde groups in glucose chains (Janson, 1967). Due to the negative charge, adsorption of cationic solutes and exclusion of anionic solutes can be observed when using the gel for gel filtration chromatography (Gelotte, 1960; Janson, 1967). The presence of sodium or potassium ion in starch gel also suggests negative charge in the gel. Some carboxylic groups might exist in starch gel, and this might cause a weak electrostatic interaction.

Table 1.2. K_{app} and D_{eff} of six seasoning compounds.

	K_{app} [-]	$D_{eff} \times 10^{10}$ [m^2/s]		$D_0 \times 10^{10}$ [m^2/s]
Glucose	0.74 ± 0.03	3.81	6.75	(Hayduk and Laudie, 1974)
Sucrose	0.66 ± 0.06	3.12	5.24	(Hayduk and Laudie, 1974)
NaCl	0.69 ± 0.02	12.0	16.0	(Handbook of chemistry, 1984)
Acetic acid	0.53 ± 0.06	9.86	11.9	(Hayduk and Laudie, 1974)
Monosodium glutamate	0.62 ± 0.09	6.82	7.0	
Vanillin	1.36 ± 0.15	4.32	6.3	

* The value of K_{app} is expressed as mean ± standard deviation (n = 5 ~ 8).

* The value of D_0 of glucose, sucrose, NaCl and acetic acid is cited from literatures.

* The value of D_0 of monosodium glutamate and vanillin is calculated applying Wilke's method (Wilke, 1949).

1.3.5. Distribution and diffusion coefficients of seasoning compounds onto starch gel

Distribution and diffusion coefficients, K_{app} and D_{eff}, of typical seasoning compounds were estimated at 25°C. Six compounds, with distinct chemical properties were used to represent typical seasoning materials. These were glucose and sucrose (non-electrolyte), NaCl (strong electrolyte), acetic acid (weak electrolyte), monosodium glutamate (amphoteric ion), and vanillin (hydrophobic substance).

The K_{app} and D_{eff} of the seasoning materials are listed in Table 1.2. The K_{app} values were lower than unity in all components except for vanillin. Although the molecular masses of NaCl, acetic acid, and monosodium glutamate were smaller than those of glucose and sucrose, their K_{app} values were lower than those of glucose and sucrose. NaCl, acetic acid, and monosodium glutamate are electrolytes, while glucose and sucrose are non-electrolytes. Therefore, any electrical interaction between NaCl, acetic acid, or monosodium glutamate and the gel would assist in their distribution onto the gel, in analogy with the above-mentioned salts. The K_{app} value of vanillin (greater than unity) suggested the effect of an unidentified interaction between the solute and the starch gel.

Greater D_{eff} values were observed for smaller compounds. The D_{eff} of a solute in a porous material was related to its diffusion coefficient in a dilute solution, D_0, using Eq. (1.6) (Westrin and Axelsson, 1991).

$$D_{eff} = (\varepsilon_p / \tau)\, D_0 \qquad (1.6)$$

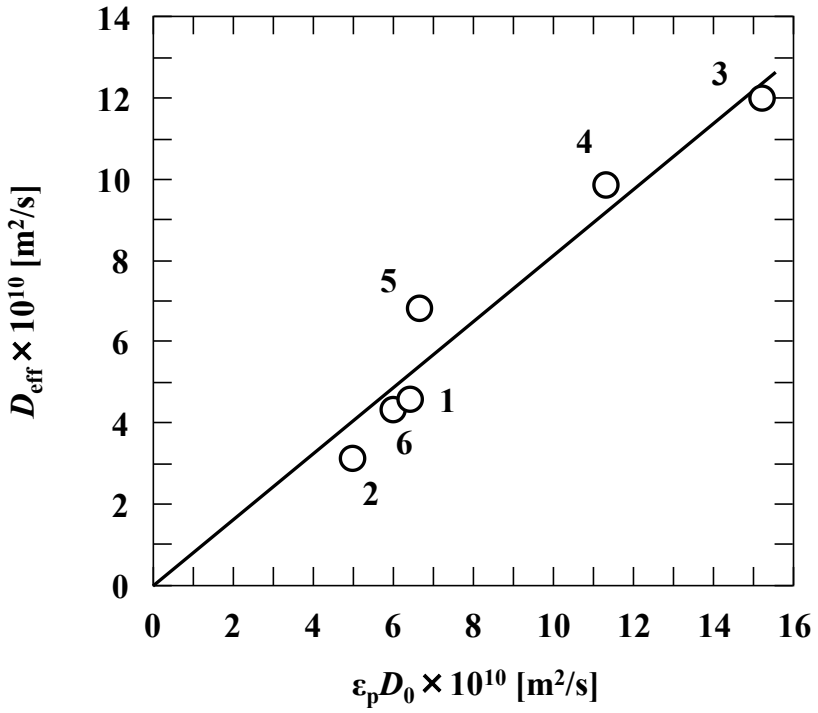

Fig. 1.7. Relationship between D_{eff} and $\varepsilon_p D_0$. Numbers represent the seasoning compounds 1: glucose, 2: sucrose, 3: NaCl, 4: acetic acid, 5: monosodium glutamate, and 6: vanillin.

Where τ denotes the tortuosity factor reflecting the effective diffusion distance. Figure 1.7 demonstrates the relationship between D_{eff} and $\varepsilon_p D_0$ for the seasoning compounds. The D_0 value of each solute was also showed in Table 1.2. The D_0 values of glucose, sucrose, acetic acid (Hayduk and Laudie, 1974) and NaCl (Handbook of chemistry, 1984) was cited from literatures, and those of monosodium glutamate and vanillin were estimated according to the Wilke's method (Wilke, 1949). Most of the plots displayed a straight line passing through the origin, and the τ value of starch gel was estimated to be 1.17 from the slope of the line. Although vanillin showed a weak adsorption onto the starch gel, the adsorption might scarcely affect the estimation of the diffusion coefficient due to low solid content and weak interaction. Possible reasons why Eq. (1.6) could be applied for all solutes is low contribution of gel skeletal on adsorption phenomena to diffusion.

The τ values of porous materials, which were used as heterogeneous catalysts, have been

previously reported to be in the range of 1.5 and 6 (Satterfield, 1970). Examples include a τ value of 2.2 for a chromatographic resin based on methacrylate polymer, TSK-HW65F (Gibbs *et al.*, 1992), and 1.88 to 2.49 for a chitosan gel cross-linked with glutaraldehyde (Krajewska and Olech, 1996). The tortuosity factor for the starch gel was much lower than these previously mentioned values, probably because of the high porosity of the gel (0.95) (Fig. 1.1).

1.4. Conclusions

The swelling pressure of the tapioca starch gel was estimated to be 1 to 3 MPa at a temperature range of 25 to 50°C, from the molar volume dependence of the apparent distribution coefficients of non-electrolytes (with different molar volumes). The swelling pressure at 60°C was lower than that at 50°C. This was ascribed to the gelatinization of the starch. The apparent distribution coefficients of electrolytes were lower than the values calculated from their molar volume and the swelling pressure of the gel. Based on the presence of alkali and alkaline earth metals in the gel, we theorize upon the role of weak electrostatic interactions on their distribution onto the gel. The apparent distribution and effective diffusion coefficients of typical seasoning compounds on the gel were measured at 25°C. The tortuosity factor of the gel was estimated to be 1.17.

Chapter 2

Swelling pressure of wet rice grains estimated from distribution coefficients of saccharides

2.1. Introduction

As shown in Chapter 1, the swelling pressure of starch gel plays an important role in the distribution equilibria of non-electrolytes. In this chapter, insight obtained from starch gel was applied to distribution of non-electrolytes onto rice, which is mainly composed with starch.

It was reported that rice grains differently rehydrated and swelled (Nakashima and Kishimoto, 2006; Sakamoto *et al.*, 2015). Thus, swelling pressure of rice during cooking could change, and this change in swelling pressure would be an important factor affecting the distribution of seasonings during preparation of flavored rice. However, the swelling pressure of rehydrated rice grains has not been estimated. In this context, we estimated swelling pressures of two cultivars of non-glutinous rice and two cultivars of sticky rice, by applying the insight obtained in Chapter 1.

2.2 Materials and methods

2.2.1. Materials

Non-glutinous rice cultivars (called "Uruchi"), Koshihikari and Yumepirika, were harvested in Shiga and Hokkaido, respectively in 2013; sticky rice cultivars (called "Mochi"), Habutaemochi and Kitayukimochi, were also harvested in Shiga and Hokkaido, respectively, in 2013. All rice varieties were purchased at a local supermarket in Kyoto. Rice materials were preserved in a refrigerator (NC-ME31A, Nihon Freezer, Tokyo) or a low-temperature room at 4°C until use. Fructose, sucrose, raffinose pentahydrate, iodine, and invertase (solution) were purchased from Wako Pure Chemical Industries (Osaka, Japan). Potato amylose was obtained from Sigma-Aldrich Japan (Tokyo) and Fructose Assay kit (ENZYTEC® *fluid* D-Fructose) was obtained from J. K. International (Tokyo). α-Galactosidase was supplied by Amano Enzyme

(Nagoya, Japan). All other chemicals were purchased from Wako.

2.2.2. Pretreatment of rice

Prior to experimental use, rice was washed as follows: approximately 20 mL of distilled water was poured onto 10 g of rice and gently stirred using a glass rod for 10 s. After discarding the water, this process was repeated twice with fresh distilled water. The washed rice was immersed in a large amount of distilled water for at least 2 h at a specific temperature using a water bath (Thermominder SM-05, Taitec, Saitama, Japan, at 25°C to 60°C, and Labbath LB-21 JR, Taitec, at 5°C to 15°C). The washed rice is hereafter referred to simply as 'rice'.

2.2.3. Measuring apparent density and porosity of rice

The apparent density of the wet rice, ρ_{app} [kg/m^3], was measured pycnometrically. The pycnometer with rice was kept at a specific temperature (5 ~ 60°C) for 30 min or longer. Prior to the measurement, the volume of the pycnometer at the specific temperature was calibrated using distilled water.

The wet rice was dried to a constant weight at 105°C for 4 days using a DN-400 oven (Yamato Scientific, Tokyo). The volumetric fraction of water within the rice was estimated from the difference in weight between the wet and dry rice and was regarded as the porosity of the rice, ε_p.

2.2.4. Estimation of swelling pressure of rice

The distribution coefficients of the different solutes into the rice were measured by an adsorption-desorption method. The wet rice (approximately 1.1 g), was precisely weighed and soaked in 30 mL of the appropriate solution. The solute concentration ranged from 5 to 150 mmol/L for fructose, from 10 to 50 mmol/L for sucrose and from 3 to 35 mmol/L for raffinose. The rice was incubated with solute for at least 5 h at a specific temperature of 5°C to 60°C to

reach distribution equilibrium and was subsequently removed from the solution. The excess solution on the rice surface was blotted away using a Kimtowel paper (Nippon Paper Crecia, Tokyo, Japan). The solute distributed into the rice was desorbed by soaking the rice in 10 mL of distilled water for at least 6 hours at the same temperature as for soaking. The concentration of desorbed solute, C_f [mol/m^3], was determined as follows: fructose concentration was determined using the fructose assay kit according to manufacturer's protocol. Sucrose and raffinose were hydrolyzed using invertase and α-galactosidase as described previous chapter (Sha and Adachi, 2015; Chapter 1), and the resulting fructose concentration was determined using the fructose assay kit.

Based on the mass balance for the solute before and after desorption, the apparent distribution coefficient, K_{app} [-], of the solute into the rice was estimated using the method mentioned in Chapter 1 (Equation (2.1)).

$$C_f = K_{app} [((W_g / \rho_{app}) / V_L] \cdot (C_0 - C_f) \quad (2.1)$$

The apparent distribution coefficient, K_{app}, of a non-electrolyte having the partial molar volume, v_s [m^3/mol], onto a polymer matrix could be related with each other using a swelling pressure, Π [Pa], of the matrix, already mentioned in Chapter 1 (Equation (2.2)),

$$K_{app} = \gamma_0 \exp[-\Pi v_S / (RT)] \quad (2.2)$$

The K_{app} values of fructose, sucrose, and raffinose were plotted against their molar volumes, which were used instead of their partial molar volumes, on the semi-logarithmic scale. The plots produce a straight line, and the Π value can be evaluated from the slope of the line (Adachi *et al.*, 1989). The molar volumes of fructose, sucrose and raffinose were 1.14×10^{-4}, 2.20×10^{-4}, and 3.25×10^{-4} m^3/mol, respectively (Adachi and Matsuno, 1997).

2.2.5. Measuring amylose content of rice

A simplified spectrophotometric method was applied to analyze the amylose content of rice (Juliano, 1971). A rice sample was ground into a powder using a mortar and a pestle, and the

powder (approximately 100 mg) was mixed with 1 mL of 95% (v/v) ethanol and 9 mL of 1 mol/L sodium hydroxide in a test tube. The mixture was incubated for 10 min at 100°C using an AHA hot plate (As One, Osaka), and then water was added to reach a final volume of 100 mL. Five mL of the solution was transferred into a clean test tube and was mixed with 1 mL of 1 mol/L acetic acid and 2 mL of iodine solution containing 0.2% (w/v) iodine and 2% (w/v) potassium iodide. Water was added to reach a final volume of 100 mL, and the absorbance of the solution was measured at 620 nm by using a UV-1200 spectrophotometer (Shimadzu, Kyoto, Japan). A calibration curve was prepared using potato amylose as a standard.

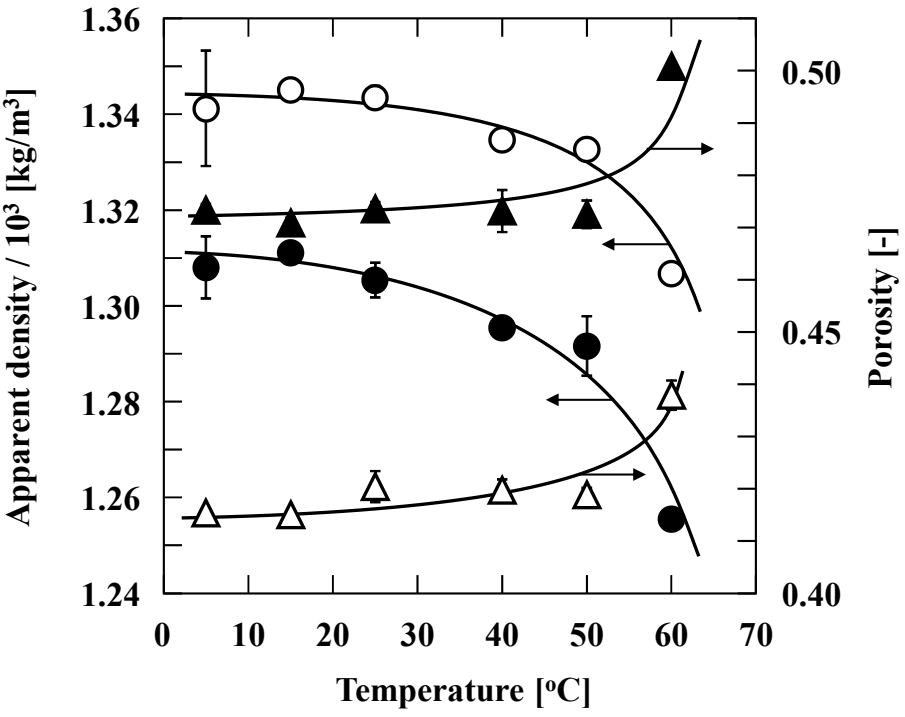

Fig. 2.1. Temperature dependence of apparent density (circles) and porosity of rice (triangles). Symbols represent apparent density of Koshihikari (open symbols) and Habutaemochi (closed symbols). Values obtained from triplicate measurements are represented as mean ± standard deviation.

2.3. Results and discussion

2.3.1. Apparent density and porosity

Figure 2.1 shows the apparent density, ρ_{app}, and porosity, ε_p, of Koshihikari and Habutaemochi cultivars, which are non-glutinous and sticky rice varieties, respectively, in the temperature range of 5°C to 60°C. The ρ_{app} value of Koshihikari was higher than that of Habutaemochi at all temperatures; while the ε_p value of the former was lower than that of the latter. The temperature did not significantly affect the ρ_{app} and ε_p values of either Koshihikari or Habutaemochi. However, the ρ_{app} values slightly decreased and ε_p values slightly increased at 60 °C, indicating that both types of rice grains swelled at this temperature. Because the gelatinization temperature of rice starch is in the range of 60°C to 75°C (Chungcharoen and Lund, 1987), the significant changes in the ρ_{app} and ε_p values at 60°C can be attributed to starch gelatinization.

Uruchi and Mochi rice types are distinguished by their different starch compositions, and the apparent amylose contents of Koshihikari, Yumepirika, Habutaemochi and Kitayukimochi were determined to be 23.0% ± 0.4%, 21.9% ± 0.5%, 6.2% ± 1.1%, and 5.8% ± 0.2% (mean ± standard deviation, n = 2), respectively. The ρ_{app} and ε_p values at 25°C are plotted against the amylose contents of the four cultivars in Fig. 2.2. The ρ_{app} values were proportional to amylose content and ε_p values were inversely proportional to the amylose content. These tendencies are in accordance with the fact that starches from low amylose cultivars can accommodate more water (Fuwa *et al.*, 1994).

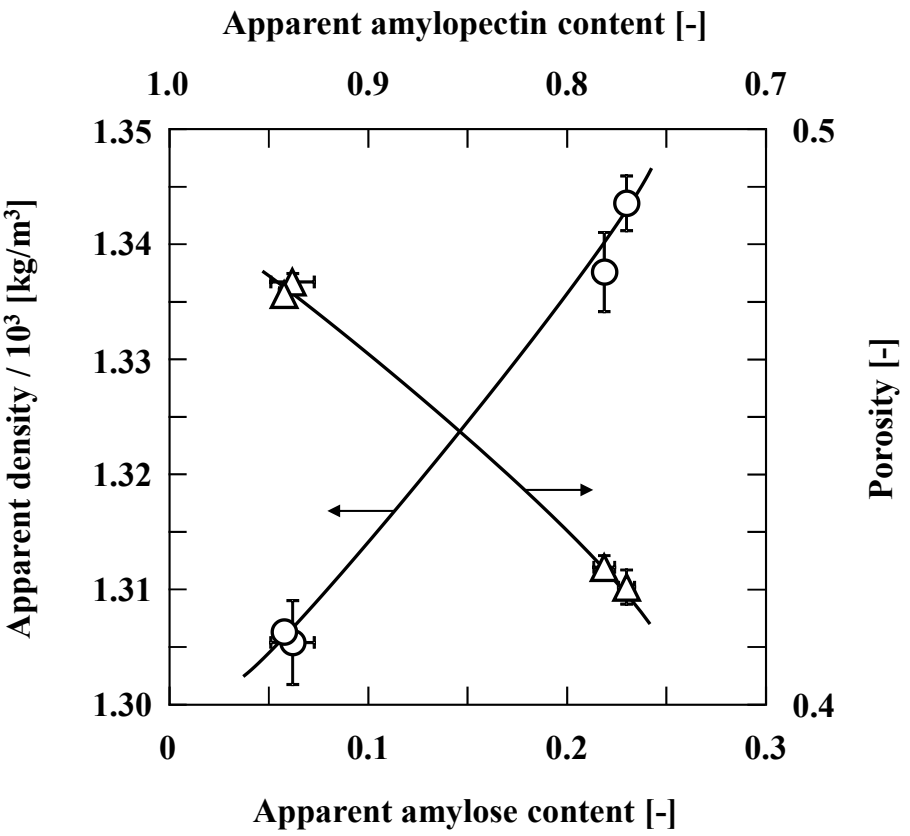

Fig. 2.2. Effects of apparent amylose content on apparent density (circles) and porosity (triangles) of rice at 25°C. Symbols from left to right represent Kitayukimochi, Habutaemochi, Yumepirika and Koshihikari, respectively. Apparent amylose content was measured in duplicate, and results are represented as mean ± standard deviation.

2.3.2. Swelling pressure of rice

The apparent distribution coefficients (K_{app}) of fructose, sucrose, and raffinose for Koshihikari and Habutaemochi cultivars were measured at 5, 25, and 50°C. According to Eq. (2.2), the K_{app} values are plotted against the molar volumes of the solutes on the semi-logarithmic scale to estimate the swelling pressures, Π, of the rice grains as shown in Fig. 2.3. The same plots were also made for Yumepirika and Kitayukimochi at 25°C (data not shown). The plots gave straight lines for all the cultivars, and the Π values at 25°C were evaluated to be 7.5, 6.3, 6.2, and 5.9 MPa for Koshihikari, Yumepirika, Habutaemochi and Kitayukimochi, respectively. The rice with higher amylose content seems to have the higher swelling pressure.

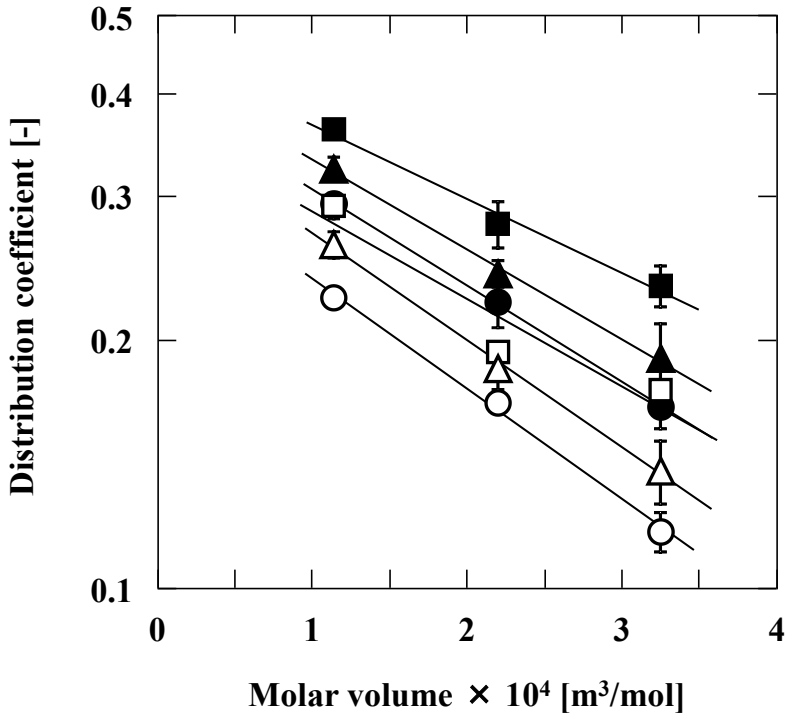

Fig. 2.3. Estimation of swelling pressures of Koshihikari (open symbols) and Habutaemochi (closed symbols) from the distribution coefficients of saccharides into rice at 5°C (circles), 25°C (triangles), and 50°C (squares).

The Π values of the wet rice grains were much larger than that of tapioca starch gel, which was 1.1 MPa at 25°C (Sha and Adachi, 2015; Chapter 1). The large Π value of the rice grains can be attributed to their varied composition.

2.3.3. Temperature effects on distribution and swelling

In order to examine the effect of temperature on swelling properties, the K_{app} value of fructose was measured for Koshihikari and Habutaemochi cultivars from 5°C to 60°C (Fig. 2.4). Relatively large standard deviations at high temperatures might come from loss of macerated rice mass during adsorption and desorption. The K_{app} value of fructose for Habutaemochi was higher than that for Koshihikari at all temperatures in this range. Similarly to the temperature dependencies of the ρ_{app} and ε_p values shown in Fig. 2.1, the K_{app} value gradually increased with

increasing temperature in the range of 5°C to 50°C, but then rapidly increased at 60°C. The rapid increase in the K_{app} at 60°C can be also attributed to the starch gelatinization of the rice. The temperature dependence of the K_{app} value was analyzed in the rage of 5°C to 50°C based on the van't Hoff's equation (Eq. (2.3)).

$$d \ln K_{app} / d (1/T) = -\Delta H / R \quad (2.3)$$

where ΔH [J/mol] is the enthalpy change for distribution. As shown in Fig. 2.4, the plots of the K_{app} values against the reciprocal of the absolute temperature gave straight lines for both Koshihikari and Habutaemochi varieties, and the ΔH values were estimated to be 4.7 and 3.5 kJ/mol, respectively, from the slopes of the lines.

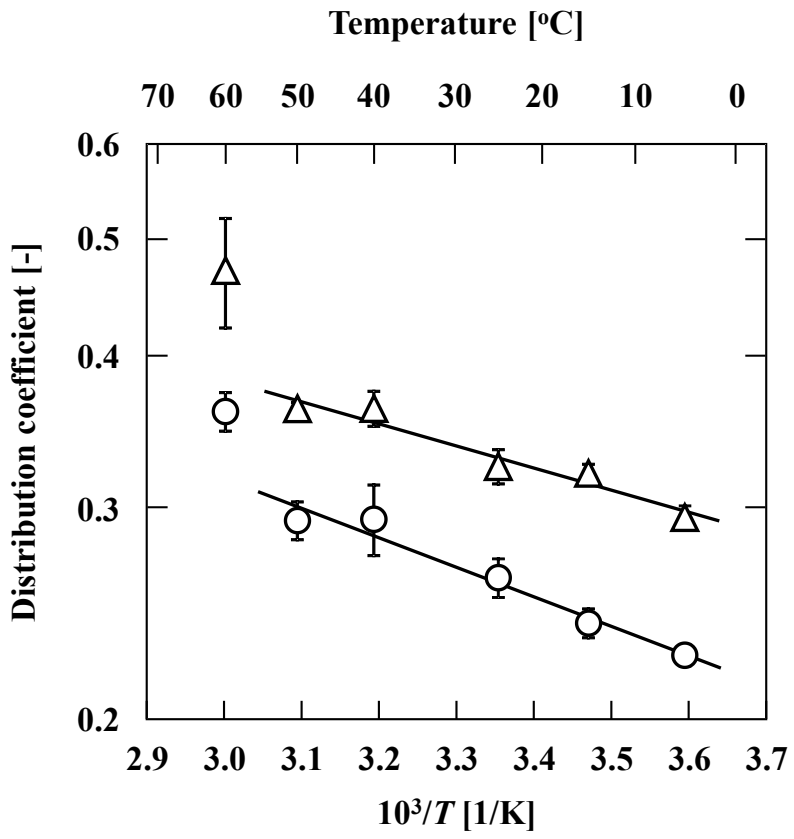

Fig. 2.4. Temperature dependence of distribution coefficient of fructose into Koshihikari (circles) and Habutaemochi (triangles). Data is represented as mean ± standard deviation for measurements at five different concentrations.

The Π values of Koshihikari and Habutaemochi were estimated from 5°C to 50°C, and are plotted against the reciprocal of the absolute temperature in Fig. 2.5. No significant temperature dependence was found for either Koshihikari or Habutaemochi. Equation (2.2) indicates that the K_{app} vale of a solute depends on both the γ_0 and Π/T values. Because the Π value did not significantly depend on the temperature, the Π/T value was smaller at higher temperatures. This would be a possible reason for the larger K_{app} value of fructose at higher temperatures (Fig. 2.4). Another possible reason for the larger K_{app} value is the change in γ_0 with temperature. Figure 2.6 shows the temperature dependence of the γ_0/ε_p value for Koshihikari and Habutaemochi cultivars. The γ_0/ε_p value of less than unity suggests that the whole interior void is not available for the solute. However, the γ_0/ε_p became larger at higher temperatures and approached unity

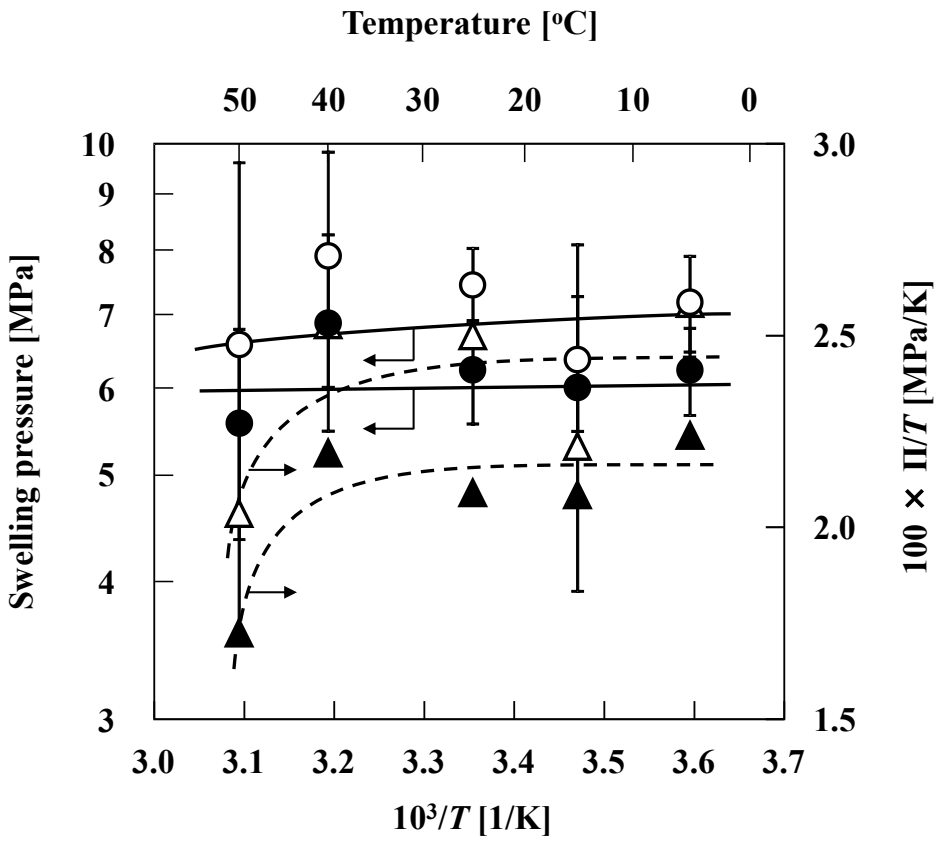

Fig. 2.5. Temperature dependence of swelling pressure (circles) and Π/T value (triangles) for Koshihikari (open symbols) and Habutaemochi (closed symbols). Error bars for swelling pressure represent 90% confidence interval.

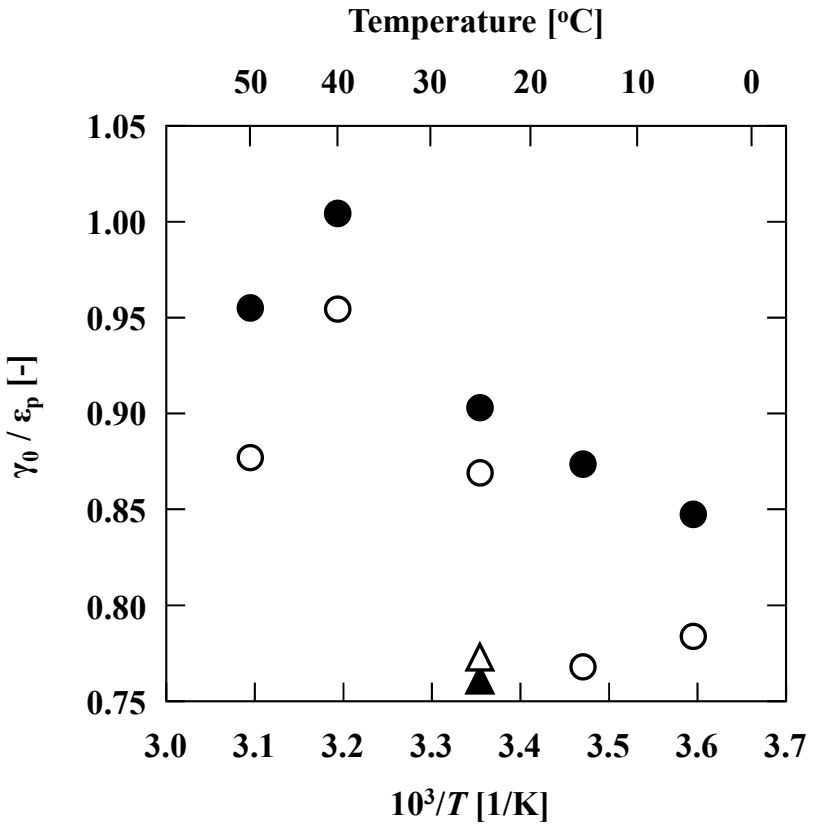

Fig. 2.6. Temperature dependence of γ_0/ε_p of Koshihikari (open circles), Habutaemochi (closed circles), Yumepirika (open triangle), and Kitayukimochi (closed triangle).

for both the cultivars. This would indicate that the rice grain structure gradually loosens and the interior volume available for distribution of solute becomes larger with the increasing temperature. The relaxation of rice structure can account for the larger K_{app} values at higher temperatures.

2.4. Conclusions

The apparent density and porosity of four rice cultivars, Koshihikari, Yumepirika, Habutaemochi, and Kitayukimochi, decreased and increased, respectively, as temperature increased from 5°C to 60°C. Large changes of these two values were observed at 60 °C, which can be ascribed to the starch gelatinization of rice. The swelling pressures of wet rice grains

were estimated to be 7.5, 6.3, 6.2, and 5.9 MPa at 25°C for Koshihikari, Yumepirika, Habutaemochi, and Kitayukimochi, respectively, from the dependency of the distribution coefficients of solutes on their molar volumes, indicating that the amylose content of each rice cultivar did not affect each swelling pressure. The distribution coefficients of fructose onto the Koshihikari and Habutaemochi were larger at higher temperatures, but the temperature dependence of the swelling pressure was not significant for both cultivars. These results suggested that the increase in the distribution coefficient was not caused by change of swelling pressure of the rice, but by the gradual relaxation of the interior structure of rice with increasing temperature.

Chapter 3

Adsorption isotherms of hydrophobic substances onto a chromatographic organic monolith

3.1. Introduction

A monolith has a three-dimensional continuous skeleton and pore structure (Nakanishi, 1997). Chromatographic columns prepared from monoliths show wider flow channels and thinner skeletons than conventional packed-bed chromatographic columns do. These two characteristics improve separation performance in chromatography. Based on the matrix material, chromatographic monoliths are classified as silica or organic monoliths. Silica monoliths have high mechanical strength (Altmaier and Cabrera, 2008), and organic monoliths can be chemically modified in various ways after preparation (Umemura *et al.*, 2008). The preparation and characterization of monoliths have been extensively investigated (Vonk *et al.*, 2014; Yang *et al.*, 2014). Besides, there are some reports concerning chromatographic separation of proteins (Teepakorn *et al.*, 2016), nucleic acids (Staňková and Jandera, 2016) or living cells (González- González *et al.*, 2016), using monoliths.

In order to use the monoliths reasonably, their adsorption characteristics with various adsorbates should be considered. However, insufficient research has been conducted on these characteristics.

In this chapter, adsorption isotherms of five adsorbates of varying degrees of hydrophobicity and having almost the same molecular mass onto a chromatographic monolith prepared from an organic polymer were measured using 50% (v/v) aqueous acetonitrile as an eluent. Equations describing the isotherms will be discussed.

3.2. Materials and methods

3.2.1. Materials

The chromatographic monolith (T85; i.d. 1.0 mm × 130 mm), which was an epoxy-based stationary phase of 1,3-bis(*N*,*N*-diglycidylaminomethyl)cyclohexane prepared using 4,4'-methylene-bis-cyclohexylamine, polyethylene glycol, and 6-(phenylamino)-1,3,5-triazine-2,4-dithiol as hardener, porogen, and metal trapping agent, respectively, was kindly supplied by Emaus Kyoto (Kyoto, Japan). Methyl *p*-hydroxybenzoate (molecular mass: 152.15 g/mol), vanillin (152.15 g/mol), 3-hydroxy-4-methoxybenzaldehyde (152.15 g/mol), coumarin (146.15 g/mol), and caffeine (194.19 g/mol), which were used as adsorbates, were purchased from Wako Pure Chemical Industries (Osaka, Japan). Methyl *p*-hydroxybenzoate and 3-hydroxy-4-methoxybenzaldehyde are called methylparaben and isovanillin, respectively. Acetonitrile used as a mobile phase was also purchased from Wako. In the estimation of column porosity, tetrahydrofuran (HPLC grade, Wako) was used as a mobile phase. Toluene and styrene were also purchased from Wako. Polystyrenes with different average molecular masses (820, 2500, 4130, 13200, 18000, 31600, 97400, and 213600 g/mol) were purchased from Sigma-Aldrich Japan (Tokyo).

3.2.2. Porosity of the column

Column porosity was estimated using inverse size-exclusion chromatography (Guan and Guiochon, 1996). Toluene, styrene, and polystyrenes with average molecular masses from 8.2 × 10^2 to 2.1 × 10^5 g/mol were used as solutes with known molecular masses.

Each solute was dissolved in tetrahydrofuran to produce 2.0 g/L solutions. The HPLC system consisted of a pump (LC-10AD$_{VP}$, Shimadzu, Kyoto), a UV detector (SPD-10AV$_{VP}$, Shimadzu), and a recorder (C-R8A, Shimadzu). The column temperature was maintained at 24.0 ± 0.5°C using a custom-made sand bath composed of a stainless steel can (i.d. 51 mm × 213 mm) and a mantle heater. A solution (1 μL) was added to the column and eluted at 0.03

mL/min. The elution profile of the solute was recorded by monitoring the absorbance at 254 nm.

3.2.3. Adsorption isotherm

The amount of adsorbate adsorbed onto the chromatographic monolith was measured by a breakthrough method. Briefly, a large amount of adsorbate solution, which was dissolved in 50% (v/v) aqueous acetonitrile at a known concentration, was loaded onto the column and eluted at 0.01 mL/min using an HPLC pump (LC-20AD, Shimadzu). Fluctuation in the flow rate was within 0.5%. Although the acetonitrile content of eluent affect the adsorption behavior (Moravcová *et al.*, 2003; Aggarwal *et al.*, 2014), the content was fixed at 50% in this study. The adsorbate concentrations were in the ranges 6.6×10^{-4} to 9.9×10^{-2} mol/L for methylparaben, 6.8×10^{-4} to 1.7×10^{-1} mol/L for coumarin, 2.0×10^{-3} to 1.3×10^{-1} mol/L for vanillin, 2.0×10^{-3} to 1.3×10^{-1} mol/L for isovanillin, and 5.2×10^{-4} to 1.0×10^{-1} mol/L for caffeine. The column temperature was maintained at 24.0 ± 0.1°C using a column oven (CTO-30A, Shimadzu). A breakthrough curve of each adsorbate was obtained by monitoring the absorbance of the eluate at 283 nm for methylparaben, 366 nm for coumarin, 345 nm for vanillin, 360 nm for isovanillin, and 300 nm for caffeine. The cell volume of the detector was 5 μL, and the dead volume of the system was estimated to be 31.3 μL from the elution behavior of toluene in the system without the column. The delay in elution time due to the dead volume was corrected in the calculation of the amount adsorbed.

The amount adsorbed, q, was calculated from the breakthrough curve obtained in each experiment using Eq. (3.1) (Jacobson *et al.*, 1984):

$$q = \frac{Qt_{\mathrm{e}}C_0 - Q\int_0^{t_{\mathrm{e}}} C\mathrm{d}t - \varepsilon_{\mathrm{ext}}VC_0}{(1-\varepsilon_{\mathrm{ext}})V} \tag{3.1}$$

where C_0 is the feed concentration of the adsorbate, Q is the volumetric flow rate (0.01 mL/min), t_{e} is the end time, V is the column volume calculated from its dimensions, and $\varepsilon_{\mathrm{ext}}$ is the external

porosity. The measurement of q at a specific C_0 was only once, but the q values for a solute were evaluated at various C_0 values. The value of ε_{ext} was assumed to be 0.65 as described later. The integration in Eq. (3.1) was conducted numerically using Simpson's method.

3.3. Results and discussion

3.3.1. Column porosity

The relationship between the molecular masses of the solutes and their retention volumes consists of two parts that correspond to channels outside the stationary phase and pores in the stationary phase (Guan and Guiochon, 1996). Figure 3.1 shows the relationship obtained using toluene, styrene, and polystyrenes with molecular masses ranging from 8.2×10^2 to 2.1×10^5 g/mol as standards. In the figure, the retention volumes were normalized by the total volume of the column. The total porosity of the column was determined to be 0.76 from the retention volume of toluene. However, an inflection point, which corresponded to external porosity, was not clearly observed. This fact might be ascribed to a small pore diameter. The ε_{ext} value is required to calculate the amount adsorbed onto the monolith. Therefore, we assumed the value of 0.65 from the intersection of two curves drawn in Fig. 3.1.

3.3.2. Adsorption isotherms

Adsorption isotherms of methylparaben, coumarin, vanillin, isovanillin, and caffeine onto the organic monolith at 24°C are shown in Fig. 3.2. The amount is expressed based on the total volume of the monolith including the pore volume. The isotherms of coumarin and caffeine were linear, and those of methylparaben, vanillin, and isovanillin were non-linear.

The linear isotherms of coumarin and caffeine were expressed by the Henry equation (3.2):

$$q = H C_0 \qquad (3.2)$$

where H is the Henry constant. The H values of coumarin and caffeine were estimated to be 1.9 and 0.53 L/L-resin, respectively.

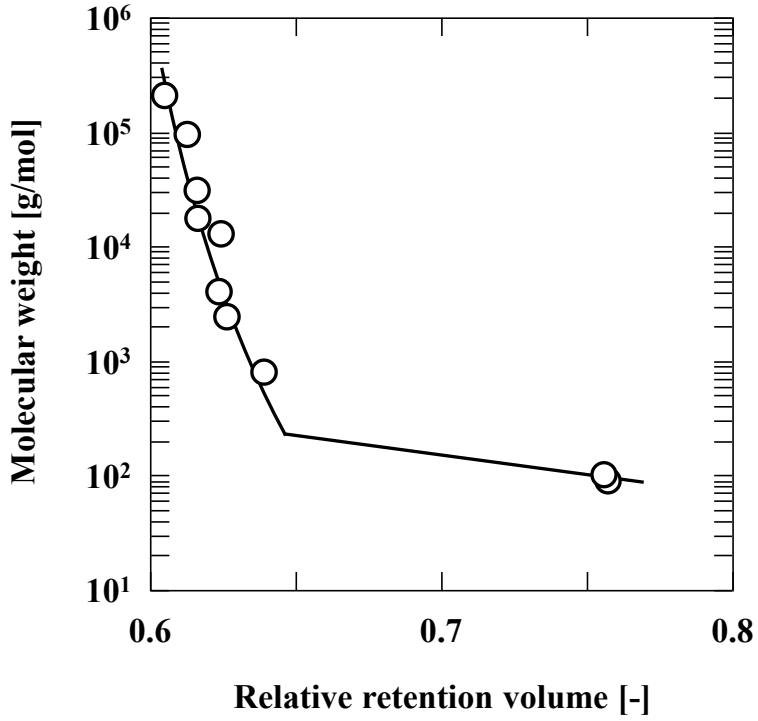

Fig. 3.1. Estimation of chromatographic organic monolith porosity by inverse size-exclusion chromatography.

The non-linear isotherms of methylparaben, vanillin, and isovanillin could not be expressed by the simple Langmuir equation, but could be expressed well by combining the Henry and Langmuir equations as shown by Eq. (3.3):

$$q = \frac{q_{\mathrm{m}} K C_0}{1 + K C_0} + H C_0 \qquad (3.3)$$

where K is the parameter reflecting the affinity of an adsorbate for the stationary phase (monolith matrix), and q_{m} is the amount of adsorbate for monolayer coverage on the surface. The first and the second terms of the right-hand side of Eq. (3.3) indicate adsorption of the adsorbate onto the stationary phase and distribution into the pores of the phase, respectively. The values of q_{m}, K, and H were estimated to obtain best-fit curves for the observed q values using Solver in Microsoft Excel. Solid curves in Fig. 3.2 were drawn using the estimated values of q_{m}, K, and H.

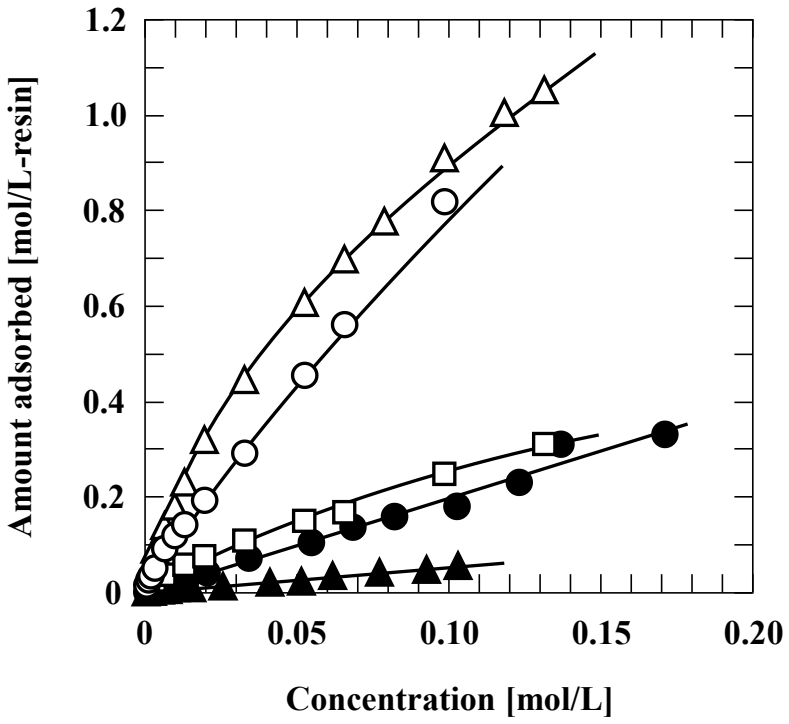

Fig. 3.2. Adsorption isotherms of methylparaben (○), vanillin (△), isovanillin (□), coumarin (●), and caffeine (▲) onto the chromatographic organic monolith at 24°C.

Table 3.1. Parameters of adsorption isotherms for each adsorbate

Adsorbate	log*P* *	q_m [mol/L-resin]	*K* [L/mol]	*H* [L/L-resin]
Methylparaben	1.96	0.043	530	7.5
Coumarin	1.39			1.9
Vanillin	1.21	0.66	30	3.9
Isovaniliin	0.97	0.043	270	2.1
Caffeine	-0.07			0.53

* The log*P* values were cited from literatures (Bondor *et al.* , 1989; Lavine *et al.* , 1994; Ishihama *et al.* , 1996).

Table 3.1 summarizes the *H* values for coumarin and caffeine, and the q_m, *K*, and *H* values for methylparaben, vanillin, and isovanillin. The log*P* values of the adsorbates (Bodor, 1989; Lavine *et al.*, 1994; Ishihama *et al.*, 1996) are also shown in the table to indicate their hydrophobicities. Although there were no correlations between the log*P* values and the

adsorption parameters, the more hydrophobic adsorbates, the isotherms of which were expressed by Eq. (3.3), tended to show larger H values. This tendency suggested that the more hydrophobic adsorbates were prone to easy distribution into the stationary phase. Adsorption onto the stationary phase was characterized by the two parameters, q_m and K. The small q_m and large K values of methylparaben and isovanillin indicated a low number of available adsorption sites for them, although their affinities for the monolith were strong. This fact indicated that the monolith had more adsorption sites for vanillin, although its affinity was weaker.

Among the five adsorbates having almost the same molecular masses, vanillin was adsorbed the most on the monolith, and methylparabene followed. Their absorbability was not correlated to their hydrophobicity although there was a tendency that more hydrophobic adsorbate was prone to more adsorption. Therefore, any specific interaction between an adsorbate and the monolith would govern the adsorption characteristics as well as the adsorbate hydrophobicity.

3.4. Conclusions

Adsorption isotherms of hydrophobic substances (methylparaben, coumarin, vanillin, isovanillin, and caffeine) onto a chromatographic organic monolith were measured at 24°C. Adsorption isotherms of coumarin and caffeine were linear and were expressed by the Henry equation. On the other hand, the isotherms of methylparaben, vanillin, and isovanillin were non-linear and could be expressed by combining the Henry and Langmuir equations. Among the adsorbates having almost the same molecular masses, vanillin was adsorbed the most on the organic monolith, and methylparabene followed. The adsorbate hydrophobicity was not a main parameter reflecting the adsorbability, but any specific interaction between the adsorbate and the monolith would play an important role on the absorbability onto the monolith.

Chapter 4

Effects of counter-ion form of a cation-exchange resin and ethanol content of eluent on the distribution coefficients of galactose, tagatose, and talose onto the resin

4.1. Introduction

Rare sugars are saccharides that occur in only small amounts in nature, and some of them have attracted attention due to their physiological functionality. Xylitol is one such rare sugar, which has an anticaries effect (Söderling *et al.*, 1989) and is contained in gum as a sweetener. D-Psicose, which is an epimer of D-fructose at the C-3 position, is very low in calories and has a beneficial effect on insulin resistance (Matsuo *et al.*, 2002; Hossain *et al.*, 2012). D-Allose, which is an epimer of D-glucose at the C-3 position, has demonstrated preventative effects in ischemia reperfusion injury and hyperpiesia. However, rare sugars are generally very expensive. The high cost restricts investigation of their physiological and textural functionalities. Because of this, the development of effective mass production processes for rare sugars is desired to promote these investigations and achieve industrialization of the production process.

Enzymatic methods for producing rare sugars (Takeshita *et al.*, 2000; Granström *et al.*, 2004; Morimoto *et al.*, 2006) have been reported, in addition to a method using anion exchange (Takamine *et al.*, 2009). We reported that isomerization of the common sugar D-galactose to D-tagatose and D-talose, which are rare sugars, was promoted in subcritical aqueous ethanol (Gao *et al.*, 2015). An enzymatic method has also been developed for the production of D-tagatose (Kim *et al.*, 2003). Isomerization in a subcritical fluid would be expected to be more effective than in conventional methods because of a higher reaction rate at higher temperature. D-Tagatose, which is a C-4 epimer of fructose, shows promise as replacement for sucrose and as a therapeutic agent against type 2 diabetes and obesity (Levin *et al.*, 1995; Lu *et al.*, 2008).

Because isomerization of D-galactose produces a mixture of unreacted substrate and the products D-tagatose and D-talose, a separation process is required to obtain the desired product,

D-tagatose. Ligand-exchange chromatography using cation-exchange resin has been commonly used in saccharide separation due to the difference in complex formation or affinity between the counter-ion of the resin and the saccharides (Goulding, 1975; Caruel *et al.*, 1991; Stefansson and Westerlund, 1996). Because water is used as an eluent, the chromatographic separation of saccharides is suitable for industrial purposes. The type of counter-ion and the divinylbenzene (DVB) content of the resin affect the separation efficiency for cation-exchange resins made from styrene cross-linked with DVB. The eluent composition also affects the separation efficiency. We reported that the ethanol content of the eluent affected the distribution coefficients of glucose, maltose and maltotriose onto the cation-exchange resin in the sodium-ion form when a mixture of ethanol and water was used as the eluent, and that the coefficients were larger at higher ethanol content in the eluent (Adachi and Matsuno; 1997).

In this study, we investigated the effects of the degree of cross-linkage of the cation-exchange resin, the counter-ion form of the resin, and the ethanol content of eluent on the apparent distribution coefficients of D-galactose, D-tagatose, and D-talose, because D-tagatose is produced from their mixture in our isomerization method using subcritical fluid.

4.2. Materials and methods

4.2.1. Materials

Cation-exchange resins with sulphonate groups and DVB contents of 6% and 8%, which were designated UBK530 and UBK550, were used in Na^+ form. They were supplied by Mitsubishi Chemical Corp., Tokyo, and the diameter of both the resins was 220 μm. D-Galactose, D-tagatose, and D-talose were purchased from Wako Pure Chemical Industries, Osaka, Japan. In this study, only D-enantiomers were used, and therefore, the prefix, D-, of all saccharides is omitted hereafter. Dextran T-110 with an average molecular mass of *ca*. 1.1×10^5, was purchased from Extrasynthase, Lyon, France, and used to estimate the bed voidage. Other chemicals were purchased from Wako or Nacalai Tesque, Kyoto, Japan.

4.2.2. Properties of the cation-exchange resin

The resins had been conditioned into the sodium form by the supplier. The resin was converted into the hydrogen-ion form according to standard procedures. The resin was packed into a cylindrical glass column at a bed height. The resin was converted into the lithium-ion form by applying a sufficient amount of 1.0 mol/L lithium chloride to the bed, and successive washing with distilled water. The bed height was recorded. The ion-form of the resin was converted to the sodium-, potassium-, calcium- and magnesium-ion form in this order by supplying 1.0 mol/L sodium, 1.0 mol/L potassium, 0.5 mol/L calcium and 0.5 mol/L magnesium chloride, respectively, and the bed height for the resin in the respective ion form was recorded.

The apparent density of each resin, ρ_{app}, was pycnometrically determined at 30°C.

Wet resin, w_w, was dried to a constant weight, w_d, in an air oven (DN400, Yamato Scientific, Tokyo, Japan) at 135°C for 5 h. The porosity of the resin, ε_p, was estimated by the following equation (Eq. (4.1)):

$$\varepsilon_p = \frac{(w_w - w_d)/\rho_w}{w_w/\rho_{app}} \tag{4.1}$$

where ρ_w is the density of water.

4.2.3. Bed shrinkage with ethanol

The cation-exchange resin in the K^+ form and with a DVB content of 8% was suspended in water and packed in the cylindrical column to give a bed height of *ca*. 25 cm, which was precisely measured. Then a 10% (v/v) ethanol solution was continuously fed into the bed until the bed height reached a constant value. After the bed height was recorded, ethanol solutions of 20, 30, and 40% (v/v) were sequentially fed into the bed and the bed height was recorded.

4.2.4. Distribution coefficient

After conversion to the Li^+, Na^+, K^+, Mg^{2+}, or Ca^{2+} form, the cation-exchange resin was packed into a cylindrical glass column of 1.5 cm inner diameter to give a bed height of *ca*. 25 cm. The bed height was precisely measured for each experiment. The air stream from a SU13 hair-dryer (Tescom Tokyo, Tokyo, Japan) connected to a desk-size programmable thermo-regulator (TXN-600, As One, Osaka, Japan) was used to maintain a column temperature of 30°C. The eluents used were distilled water or an ethanol-water mixture, the ethanol content of which was in the range of 10 to 40% (v/v). For the eluent of any ethanol content, the resin pre-equilibrated with the eluent was packed to give a bed height of *ca*. 25 cm. Solute solution, 0.5 mL of 1.0% (w/v), was applied to the bed, and was then eluted with eluent supplied by an MP-3N peristaltic pump (Tokyo Rikakiki, Tokyo, Japan) at a flow rate of 1.5 to 3.5 mL/min. When the eluent was water or 10% (v/v) ethanol, the elution profile of the solute was monitored with a YRD-883 refractometer (Shimamuratech, Tokyo, Japan) and recorded with a GL-220 data logger (Graphtech, Kanagawa, Japan). For eluent compositions of 20 to 40% (v/v) ethanol, the effluent from the column was fractionated at regular time intervals of 80 and 40 s for the flow rates of 1.5 and 2.7 mL/min, respectively. When dextran T-110 was used as the solute to estimate the bed voidage, the intervals for fractionation were 40 and 20 s for the flow rates. The liquid in the fractions was evaporated at 70°C in a DN400 oven (Yamato Scientific, Saitama, Japan) under reduced pressure with an A-1000S aspirator (Tokyo Rikakikai, Tokyo, Japan). The dried solute was dissolved in 0.1 mL water, and the solute concentration was determined using an HPLC system consisting of an LC-10ADVP pump, an RID-10A refractometer and a C-R6A chromatogram recorder (Shimadzu, Kyoto, Japan).

The apparent distribution of the solute, K_{app}, was determined by a moment analysis of the elution curve (Adachi and Matsuno, 1997; Hashimoto, 2005). The normalized first-order statistical moment, μ_1', is defined by Eq. (4.2a) and is related to K_{app} by Eq. (4.2b).

$$\mu_1' = \int_0^\infty tCdt / \int_0^\infty Cdt \quad (4.2a)$$

$$= (Z/u_0)[\varepsilon_b + (1-\varepsilon_b)K_{app}] \quad (4.2b)$$

where C is the solute concentration, t is the time, u_0 is the superficial velocity, Z is the bed height, and ε_b is the bed voidage. Because of its large molecular size, the K_{app} of dextran T-110 is zero. Therefore, it was used for determination of the bed voidage. The K_{app} values of galactose, tagatose and talose were determined from the plots of the μ_1' values against the Z/u_0 values.

4.3. Results and discussion

4.3.1. Effects of counter-ion form on the resin properties

Table 4.1 lists the densities and porosities of the resins in various ion-forms. For the resins in the same ion-form, the resin with the 8% DVB content had higher density and smaller porosity than that with 6% DVB content. The trend was that the larger ion showed higher density and smaller porosity.

Table 4.1. Propersies of resin in various ion forms*

DVB [%]	6			8		
Ion form	Relative bed height**	Density [g/mL]	Porosity	Relative bed height**	Density [g/mL]	Porosity
H^+		1.135	0.726		1.19	0.693
Li^+	0.988	1.203	0.741	0.988	1.219	0.668
Na^+	0.908	1.206	0.675	0.919	1.269	0.644
K^+	0.856	1.231	0.661	0.869	1.389	0.574
Mg^{2+}	0.864	1.223	0.689	0.907	1.251	0.653
Ca^{2+}	0.800	1.226	0.656	0.861	1.303	0.629

* Eluent used was water.

** The ratio in bed height of the resin in any ion-form to that in the hydrogen-ion form.

Table 4.2. Apparent distribution coefficients of galactose, tagatose and talose to the resin in various ion forms*

DVB [%]		6				8		
Ion form	ε_b**	Galactose	Tagatose	Talose	ε_b**	Galactose	Tagatose	Talose
Li^+	0.395	0.320	0.301	0.441	0.387	0.206	0.173	0.293
Na^+	0.398	0.427	0.356	0.641	0.378	0.333	0.257	0.560
K^+	0.382	0.514	0.395	0.711	0.395	0.415	0.299	0.639
Mg^{2+}	0.385	0.294	0.252	0.364	0.379	0.181	0.162	0.255
Ca^{2+}	0.402	0.418	0.791	1.765	0.390	0.307	0.662	1.633

* Eluent used was water.

** Voidage of the bed packed with each resin.

4.3.2. Distribution coefficients on cation-exchange resins of various ion forms

The K_{app} values of galactose, tagatose and talose onto the resins in various ion-forms are listed in Table 5.2 as well as the bed voidage ε_b. The eluent used was water. The K_{app} values of tagatose and talose were larger for the resins with both 6% and 8% DVB contents in the order Mg^{2+}, Li^+, Na^+, K^+, and Ca^{2+}, while the values for galactose were in the order $Mg^{2+} < Li^+ < Ca^{2+}$, Na^+ and K^+ for the resins with 6% and 8% DVB contents. The differences in the K_{app} values among the three solutes were the largest for the resin in the Ca^{2+} form, and next largest for the resin in the K^+ form. The K_{app} values, or the difference in the K_{app} values, reflect the mean residence times of the solutes, that is, they are equilibrium parameters. The practical separation process includes another important parameter related to rate process, that is, the sharpness and symmetry of the chromatograms.

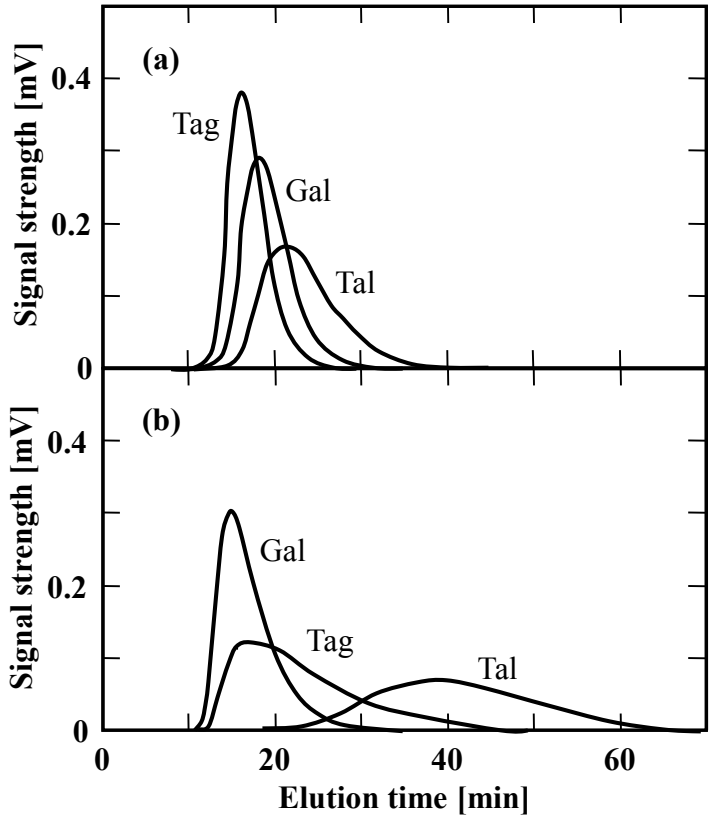

Fig. 4.1. Elution profiles of galactose (labeled Gal), tagatose (Tag) and talose (Tal) for the resins in the (a) K^+ and (b) Ca^{2+} forms with 8% DVB content at 30°C. The eluent used was water.

Figures 4.1(a) and (b) show the elution profiles of the three solutes for the resins in the K^+ and Ca^{2+} forms, respectively, with 8% DVB content. Distilled water was used as the eluent. The chromatograms for the resin in the Ca^{2+} form were broader and more asymmetrical than those for the resins in the K^+ form. The resin with the higher DVB content did not shrink significantly in comparison to the resin with low DVB content at high solute or alcohol concentration (Adachi and Matsuno, 1997). Therefore, the resin in the K^+ form with 8% DVB content was selected to be the most effective for the separation of the three solutes.

4.3.3. Effects of the ethanol content of the eluent on the distribution coefficients onto the resin of K^+ form

The effects of the ethanol content of the eluent on the bed shrinkage and the K_{app} values of galactose, tagatose, and talose were examined for the resin in the K^+ form with 8% DVB content at 30°C (Fig. 4.2). As the ethanol content of the eluent was increased, the shrinkage of the bed increased. The K_{app} values for all three solutes increased when the ethanol content of the eluent was increased. On the other hand, as the ethanol content increased, the difference in the K_{app} values between galactose and tagatose became larger, while the difference in the K_{app} values between talose and galactose became smaller. The solute with the smaller K_{app} is eluted at the shorter residence time, and the peak becomes sharper (Hashimoto, 2005). Therefore, when the three solutes are chromatographically separated from the reaction mixture obtained by the treatment of galactose in the subcritical aqueous ethanol, the removal or evaporation of the ethanol from the mixture is recommended prior to the separation. Removal of the ethanol would result in an increase in solute concentrations. Evaluation of the parameters related to the intra- and inter-particle diffusion processes of the solutes would be further required in order to reasonably design the separation process.

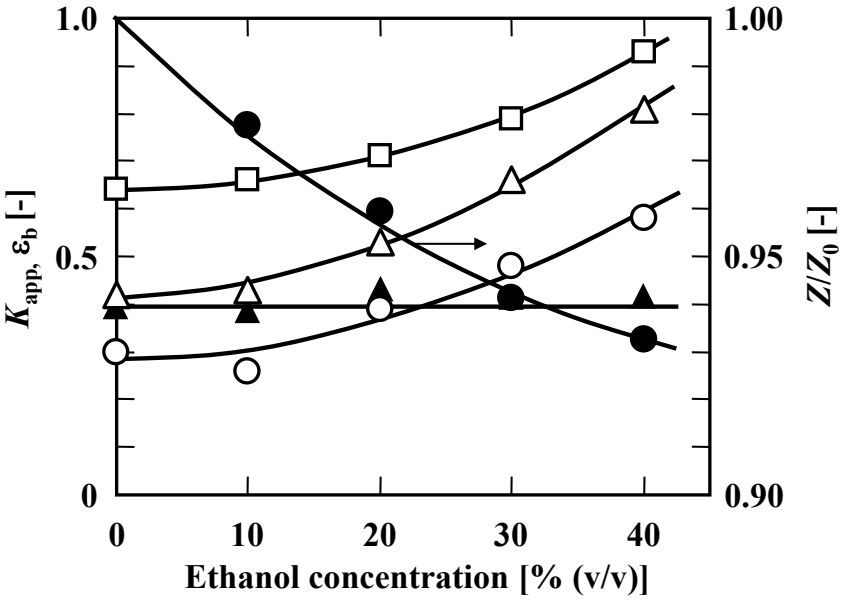

Fig. 4.2. Relative bed height, Z/Z_0 (●), bed voidage, ε_b (▲), and the K_{app} values for galactose (△), tagatose (○) and talose (□) for eluent containing different ethanol content for the resin in the K^+ form with 8% DVB content at 30°C.

4.4. Conclusions

Optimum conditions for chromatographic separation, at 30°C, of galactose, tagatose, and talose were determined by investigation of the effects of the counter-ion form of cation-exchange resin and the ethanol content of eluent on the distribution coefficients of the monosaccharides onto the resin. Resin in the K^+ form with a divinylbenzene content of 8% was found to be most suitable for the separation. The distribution coefficients of all the solutes on the resin were increased as the ethanol content of eluent increased.

Concluding remarks

Chapter 1

The apparent density and porosity of a tapioca starch gel was decreased and increased, respectively, as temperature increased from 25°C to 80°C. The distribution coefficients, K_{app}, of non-electrolytes of different molecular masses on the starch gel were measured at various temperature (from 25°C to 60°C). The swelling pressure of the gel was estimated from the coefficients at each temperature, and was observed to increase from 1 MPa to 3 MPa with a temperature increase from 25°C to 50°C. However, its value decreased at 60°C. The temperature dependency of the swelling pressure suggested the significant effect of gelatinization on the distribution equilibrium of a solute on the starch gel. The experimentally observed K_{app} values of electrolytes (0.5 to 0.8) were lower than the values calculated using the swelling pressure and specific molecular volumes of the electrolytes.

Chapter 2

The apparent density and porosity of four rice cultivars, Koshihikari, Yumepirika, Habutaemochi, and Kitayukimochi, decreased and increased, respectively, with the increasing temperature in the range of 5°C to 60°C. Especially large changes in both apparent density and porosity were observed at 60°C, which can be ascribed to the starch gelatinization of rice. The swelling pressures of wet rice grains were estimated to be 7.5, 6.3, 6.2, and 5.9 MPa at 25°C for Koshihikari, Yumepirika, Habutaemochi, and Kitayukimochi, respectively, from the distribution coefficients of solutes with different molar volumes. Rice grains having higher amylose content exhibited a weak tendency toward higher swelling pressure. The distribution coefficients of fructose for the Koshihikari and Habutaemochi cultivars were larger at higher temperatures, but the temperature dependence of the swelling pressure was not significant for both cultivars.

Chapter 3

Adsorption isotherms of hydrophobic substances (methylparaben, coumarin, vanillin, isovanillin and caffeine) onto a chromatographic organic monolith were measured at 24°C. Adsorption isotherms of coumarin and caffeine were linear and were expressed by the Henry equation. On the other hand, the isotherms of methylparaben, vanillin, and isovanillin were non-linear and could be expressed by combining the Henry and Langmuir equations. Among the adsorbates having almost the same molecular masses, vanillin was adsorbed the most on the organic monolith, and methylparabene followed. The adsorbate hydrophobicity was not a main parameter reflecting the adsorbability, but any specific interaction between the adsorbate and the monolith would play an important role on the absorbability onto the monolith.

Chapter 4

Optimum conditions for chromatographic separation, at 30°C, of galactose, tagatose, and talose were determined by investigation of the effects of the counter-ion form of cation-exchange resin and the ethanol content of eluent on the distribution coefficients of the monosaccharides onto the resin. Resin in the K^+ form with a divinylbenzene content of 8% was found to be most suitable for the separation. The distribution coefficients of all the solutes on the resin were increased as the ethanol content of eluent increased.

Acknowledgments

The author, Yuki Sha, would like to express the deepest appreciation to Professor Shuji Adachi. Extensive discussion and constructive advice given by him has been a great help in all my research work.

Also, I am indebt to Associate Professor Kyuya Nakagawa and Assistant Professor Takashi Kobayashi. Without their concrete suggestions and appropriate feedback for my experiments, this work would not have been possible.

I express gratitude to Emaus Kyoto (Kyoto) for preparing and supplying the chromatographic monolith (in Chapter 3) and Mitsubishi Chemical Corp. (Tokyo) for supplying the chromatographic resins (in Chapter 4).

References

S. Adachi and R. Matsuno: Effect of eluent composition on the distribution coefficient of saccharides on to a cation-exchange resin in sodium-form. *Biosci. Biotechnol. Biochem.*, **61**, 1296-1301 (1997).

S. Adachi, T. Watanabe and M. Kohashi: Role of swelling pressure on distribution coefficient of maltooligosaccharide in a cation-exchange resin. *Agric. Biol. Chem.*, **53**, 3203-3208 (1989).

P. Aggarwal, J. S. Lawson, H. D. Tolley and M. L. Lee: High efficiency polyethylene glycol diacrylate monoliths for reversed-phase capillary liquid chromatography of small moleccules. *J. Chromatogr. A*, **1364**, 96-106 (2014).

A. M. Ahhmed, S. Kawahara, K. Ohta, K. Nakade, T. Soeda and M. Muguruma: Differentiation in improvements of gel strength in chicken and beef sausages induced by transglutaminase. *Meat Sci.*, **76**, 455-462 (2007).

A. M. Ahhmed, T. Nasu, D. Q. Huy, Y. Tomisaka, S. Kawahara and M. Muguruma: Effect of microbial transglutaminase on the natural actomyosin cross-linking in chicken and beef. *Meat Sci.*, **82**, 170-178 (2009).

S. Altmaier and K. Cabrera: Structure and performance of silica-based monolithic HPLC columns. *J. Sep. Sci.*, **31**, 2551-2559 (2008).

H.-D. Belitz and H. Wieser, H: Bitter compounds: occurrence and structure-activity relationship. *Food Rev. Int.*, **1**, 271-354 (1985).

N. Bodor, Z. Gabanyi and C.-K. Wong: A new method for the estimation of partition coefficient. *J. Am. Chem. Soc.*, **111**, 3783-3786 (1989).

V. L. Campo, D. F. Kawano, D. B. De Silva and I. Carvalho: Carrageenans: biological properties, chemical modifications and structural analysis–a review. *Carbohydr. Polym.*, **77**, 167-180 (2009).

H. Caruel, L. Rigal and A. Gaset: Carbohydrate separation by ligand-exchange liquid chromatography: Correlation between the formation of sugar-cation complexes and the elution order. *J. Chromatogr. A*, **558**, 89-104 (1991).

A. Chungcharoen and D. B. Lund: Influence of solutes and water on rice starch gelatinization. *Cereal Chem.*, **64**, 240-243 (1987).

G. A. De Ruiter and B. Rudolph: Carrageenan biotechnology. *Trends Food Sci. Technol.*, **8**, 389-395 (1997).

G. Djelveh and J. B. Gros: Measurement of effective diffusivities of ionic and non-ionic solutes through beef and pork muscles using a diffusion cell. *Meat Sci.*, **23**, 11-20 (1988).

E. Doi: Gels and gelling of globular proteins. *Trends Food Sci. Technol.*, **4**, 1-5 (1993).

J.-C. Eliasson: Interactions between starch and lipids studied by DSC. *Thermochim. Acta*, **246**, 343-356 (1994).

N. Fatin-Rouge, A. Milon, J. Buffle, R. Goulet and A. Tessier: Diffusion and partitioning of solutes in agarose hydrogels: the relative influence of electrostatic and specific interactions. *J. Phys. Chem. B*, **107**, 12126-12137 (2003).

A. L. Fox: The relationship between chemical constitution and taste. *Genetics*, **18**, 115-120 (1932).

H. Fuwa, M. Asaoka, H. Shintani, T. Shigematsu, M. Oshiba, and N. Inouchi: Properties of endosperm starch of new types of rice grains – Giant-embryo, fragrance, high-amylose, low-amylose and big-grain rice–. *Nippon Shokuhin Kogyo Gakkaishi*, **41**, 413-418 (1994).

P. Gacesa: Alginates. *Carbohydr. Polym.*, **8**, 161-182 (1988).

D. M. Gao, T. Kobayashi and S. Adachi: Production of rare sugars from common sugars in subcritical aqueous ethanol. *Food Chem.*, **175**, 465-470 (2015).

B. Gelotte: Studies on gel filtration: sorption properties of the bed material sephadex. *J. Chromatogr.*, **3**, 330-342 (1960).

J. A. Gerrard: Protein-protein cross-linking in food: methods, consequences, applications.

Trends Food Sci. Technol., **13**, 391-399 (2002).

S. J. Gibbs, E. N. Lightfood and T. W. Root: Protein diffusion in porous gel filtration chromatography media studied by pulsed field gradient NMR spectroscopy. *J. Phys. Chem.*, **96**, 7458-7462 (1992).

M. González-González, J. González-Valdez, K. Mayolo-Deloisa and M. Rito-Palomares: Monolithic chromatography: insights and practical perspectives. *J. Chem. Technol. Biotechnol.*, doi: 10.1002/jctb.5040 (2016).

R. W. Goulding: Liquid chromatography of sugars and related polyhydric alcohols on cation exchangers. *J. Chromatogr.*, **103**, 229-239 (1975).

T. B. Granström, G. Takata, M. Tokuda and K. Izumori: Izumoring: A novel and complete strategy for bioproduction of rare sugars. *J. Biosci. Bioeng.*, **97**, 89-94 (2004).

H. Guan and G. Guiochon: Study of physico-chemical properties of some packing materials. I. Measurements of the external porosity of packed columns by inverse size-exclusion chromatography. *J. Chromatogr. A*, **731**, 27-40 (1996).

A. Handa, K. Takahashi, N. Kuroda and G. W. Froning: Heat-induced egg white gels as affected by pH. *J. Food Sci.*, **63**, 403-407 (1998).

K. Hashimoto: "Chromatographic Separation Engineering (in Japanese)," Baifukan, Tokyo, pp. 26-27, 64-66 (2005).

H. Hatta, N. Kitabatake and E. Doi: Turbidity and hardness of a heat-induced gel of hen egg ovalbumin. *Agric. Biol. Chem.*, **50**, 2083-2089 (1986).

W. Hayduk and H. Laudie: Prediction of diffusion coefficients for nonelectrolytes in dilute aqueous solutions. *AIChE J.*, **20**, 611-615 (1974).

S. B. Horowitz and I. R. Fenichel: Solute diffusional specificity in hydrogen-bonding systems. *J. Phys. Chem.*, **68**, 3378-3385 (1964).

A. Hossain, F. Yamaguchi, T. Matsunaga, Y. Hirata, K. Kamitori, Y. Dong, L. Sui, I. Tsukamoto, M. Ueno and M. Tokuda: Rare sugar D-psicose protects pancreas β-islets and thus

improves insulin resistance in OLETF rats. *Biochem. Biophys. Res. Commun.*, **425**, 717-723 (2012).

N. Ishibashi, I. Ono, K. Kato, T. Shigenaga, I. Shinoda, H. Okai and S. Fukui: Role of hydrophobic amino acid residue in the bitterness of peptides. *Agric. Biol. Chem.*, **52**, 91-94 (1988).

Y. Ishihama, Y. Oda and N. Asakawa: A hydrophobicity scale based on the migration index from microemulsion electrokinetic chromatography of anionic solutes. *Anal. Chem.*, **68**, 1028-1032 (1996).

J. Jacobson, J. Frenz and C. Horváth: Measurement of adsorption isotherms by liquid chromatography. *J. Chromatogr.*, **316**, 53-68 (1984).

J.-C. Janson: Adsorption phenomena on sephadex®. *J. Chromatogr.*, **28**, 12-20 (1967).

B. O. Juliano: Simplified assay for milled-rice amylose. *Cereal Sci. Today*, **16**, 334 (1971).

K. Kato and K. Matsuda: Studies on the chemical structure of konjac mannan. Part I. Isolation and characterization of oligosaccharides from the partial acid hydrolyzate of the mannan. *Agric. Biol. Chem.*, **33**, 1446-1453 (1969).

H. J. Kim, S. A. Ryu, P. Kim and D. K. Oh: A feasible enzymatic process for D-tagatose production by an immobilized thermostable l-arabinose isomerase in a packed-bed bioreactor. *Biotechnol. Prog.*, **19**, 400-404 (2003).

B. Krajewska and A. Olech: Pore structure of gel chitosan membranes. I. Solute diffusion measurements. *Polym. Gels Networks*, **4**, 33-43 (1996).

C. Kuraishi, K. Yamazaki and Y. Susa: Transglutaminase: its utilization in the food industry. *Food Rev. Int.*, **17**, 221-246 (2001).

B. K. Lavine, S. Hendayana and J. Tetreault: Selectivity in micellar reversed-phase liquid chromatography: C-18 and C-8 alkyl bonded phases. *Anal. Chem.*, **66**, 3458-3465 (1994).

G. V. Levin, L. R. Zehner, J. P. Saunders and J. R. Beadle: Sugar substitutes: their energy values, bulk characteristics, and potential health benefits. *Am. J. Clin. Nutr.*, **62**, 1161-1168 (1995).

Y.-H. Li and S. Gregory: Diffusion of ions in sea water and in deep-sea sediments. *Geochim. Cosmochim. Acta*, **38**, 703-714 (1974).

Y. Lu, G. V. Levin and T. W. Donner: Tagatose, a new antidiabetic and obesity control drug. *Diabetes Obes. Metab.*, **10**, 109-134 (2008).

K. Maekaji: The mechanism of gelation of konjac mannan. *Agric. Biol. Chem.*, **38**, 315-321 (1974).

T. Matsuo, H. Suzuki, M. Hashiguchi and K. Izumori: D-Psicose is a rare sugar that provides no energy to growing rats. *J. Nutr. Sci. Vitaminol.*, **48**, 77-80 (2002).

D. Moravcová, P. Jandera, J. Urban and J. Planeta: Characterization of polymer monolithic stationary phases for capillary HPLC. *J. Sep. Sci.*, **26**, 1005-1016 (2003).

K. Morimoto, C. S. Park, M. Ozaki, K. Takeshita, T. Shimonishi, T. B. Granström, G. Takata, M. Tokuda and K. Izumori: Large scale production of D-allose from D-psicose using continuous bioreactor and separation system. *Enzyme Microb. Technol.*, **38**, 855-859 (2006).

M. Motoki and K. Seguro: Transglutaminase and its use for food processing. *Trends Food Sci. Technol.*, **9**, 204-210 (1998).

K. Nakanishi: Pore structure control of silica gels based on phase separation. *J. Porous Mat.*, **4**, 67-112 (1997).

K. Nakanishi, S. Adachi, S. Yamamoto, R. Matsuno, A. Tanaka and T. Kamikubo: Diffusion of saccharides and amino acids in cross-linked polymers. *Agric. Biol. Chem.*, **41**, 2455-2462 (1977).

K. Nakashima and R. Kishimoto: Water absorption and characteristics of unpolished glutinous purple rice. *J. Cookery Sci. Jpn.*, **39**, 227-232 (2006).

A.-L. Nguyen and J. H. T. Luong: Diffusion in κ-carrageenan gel beads. *Biotechnol. Bioeng.*, **28**, 1261-1267 (1986).

S. Odake, K. Hatae, A. Shimada and S. Iibuchi: Apparent diffusion coefficient of sodium

chloride in cubical agar gel. *Agric. Biol. Chem.*, **54**, 2811-2817 (1990).

W. Pigman (Ed.): "The carbohydrates: chemistry and biochemistry, 2nd Ed." Academic Press, New York, USA, p.483 (1970).

A. C. F. Ribeiro, O. Ortona, S. M. N. Simões, C. I. A. V. Santos, P. M. R. A. Prazeres, A. J. M. Valente, V. M. M. Lobo and H. D. Burrows: Binary mutual diffusion coefficients of aqueous solutions of sucrose, lactose, glucose, and fructose in the temperature range from (298.15 to 328.15) K. *J. Chem. Eng. Data*, **51**, 1836-1840 (2006).

K. Sakamoto, S. Morii, and M. Ueda: Difference in water absorption of rice in warm and cold water. *J. Cookery Sci. Jpn.*, **48**, 193-199 (2015).

C. N. Satterfield: "Mass transfer in heterogeneous catalysis," MIT Press, Cambridge, MA, p.157 (1970).

Y. Sha and S. Adachi: Swelling pressure of tapioca starch gel. *Food Sci. Technol. Res.*, **21**, 509-515 (2015).

E. Söderling, K. K. Mäkinen, C.-Y. Chen, H. R. Jr. Pape, W. Loesche and P.-L. Mäkinen: Effect of sorbitol, xylitol, and xylitol/sorbitol chewing gums on dental plaque. *Caries Res.*, **23**, 378-384 (1989).

M. Staňková and P. Jandera: Dual retention mechanism in two-dimensional LC separations of barbiturates, sulfonamides, nucleic bases and nucleosides on polymethacyrate zwitterionic monolithic micro-column. *Chromatographia*, **79** (11), 657-666 (2016).

M. Stefansson and D. Westerlund: Ligand-exchange chromatography of carbohydrates and glycoconjugates. *J. Chromatogr. A*, **720**, 127-136 (1996).

S. Takamine, T. Iida, K. Okuma, T. Shimonishi, K. Izumori and T. Matsuo: Method for producing sugar composition containing definite amount of target hexose and having sugar composition ratio different from starting sugar material, and use of sugar composition thus produced. Japanese Patent 2009-081976 (WO 2010/113785 A1) (2009).

K. Takeshita, A. Suga, G. Takada and K. Izumori: Mass production of D-psicose from D-

fructose by a continuous bioreactor system using immobilized D-tagatose 3-epimerase. *J. Biosci. Bioeng.*, **90**, 453-455 (2000).

H. Tanaka, M. Matsumura and I. A. Veliky: Diffusion characteristics of substrates in Ca-alginate gel beads. *Biotechnol. Bioeng.*, **26**, 53-58 (1984).

C. Teepakorn, K. Fiaty and C. Charcosset: Comparison of membrane chromatography and monolith chromatography for lactoferrin and bovine serum albumin separation. *Processes*, **4**, 31-43 (2016).

M. Turhan and G. Kaletunç: Modeling of salt diffusion in white cheese during long-term brining. *J. Food Sci.*, **57**, 1082-1085 (1992).

T. Umemura, N. Kojima and Y. Ueki: Development of high-throughput analysis system using highly-functional organic polymer monoliths (in Japanese). Bunseki Kagaku, **57**, 517-529 (2008).

R. J. Vonk, A. Vaast, S. Eeltink and P. J. Schoenmakers: Titanium-scaffolded organic-monolithic stationary phases for ultra-high-pressure liquid chromatography. *J. Chromatogr. A*, **1359**, 162-169 (2014).

B. A. Westrin and A. Axelsson: Diffusion in gels containing immobilized cells: a critical review. *Biotechnol. Bioeng.*, **38**, 439-446 (1991).

B. A. Westrin, A. Axelsson and G. Zacchi: Diffusion measurement in gels. *J. Controlled Release*, **30**, 189-199 (1994).

C. R. Wilke: Estimation of liquid diffusion coefficients. *Chem. Eng. Progr.*, **45**, 218-224 (1949).

P. Yang, W. Wang, X. Xiao and L. Jia: Hydrothermal preparation of hybrid carbon/silica monolithic capillary column for liquid chromatography. *J. Sep. Sci.*, **37**, 1911-1918 (2014).

H. Zhang, M. Yoshimura, K. Nishinari, M. A. K. Williams, T. J. Foster and I. T. Norton: Gelation behavior of konjac glucomannan with different molecular weights. *Biopolymers*, **59**, 38-50 (2001).

List of publications

Y. Sha and S. Adachi: Swelling pressure of tapioca starch gel estimated from distribution coefficients of non-electrolytes. *Food Sci. Technol. Res.*, **21** (4), 509-515 (2015).

Y. Sha and S. Adachi: Swelling pressure of wet rice grains estimated from distribution coefficients of saccharides. *J. Appl. Glycosci*., **63** (2), 47-50 (2016).

Y. Sha, U. Aimoto and S. Adachi: Adsorption isotherms of hydrophobic substances onto a chromatographic organic monolith. *Jpn. J. Food Eng.*, **16** (2), 167-170 (2015).

A. Tamura, Y. Sha and S. Adachi: Effects of counter-ion form of a cation-exchange resin and ethanol content of eluent on the distribution coefficients of galactose, tagatose, and talose onto the resin. *Food Sci. Technol. Res.*, **22** (2), 205-208 (2016).

Special thanks

General financial supporter

Shoto Sha

General mental supporter

Takayo Sha

Chitchatting partners in dairy life

Koki Sha

Shinki Sha

Assistant administrative staff

(*Secretary in Laboratory of Bioengineering*)

Rumiko Kamiya